Gene 809 (2022) 146048

Contents lists available at ScienceDirect

Gene

journal homepage: www.elsevier.com/locate/gene

Research paper

sRNA chaperone Hfq controls bioluminescence and other phenotypes through Qrr1-dependent and -independent mechanisms in *Vibrio fischeri*

Jovanka Tepavčević [a,*], Kaiti Yarrington [c], Brittany Fung [b], Xijin Lin [a], Karen L. Visick [b]

[a] Department of Biology, Wheaton College, Wheaton, IL, USA
[b] Department of Microbiology and Immunology, Loyola University Chicago, Maywood, IL, USA
[c] Department of Microbiology and Immunology, Carver College of Medicine, University of Iowa, Iowa City, IA, USA

ARTICLE INFO

Edited by X. Carette

Keywords:
Hfq
Vibrio fischeri
Bioluminescence
Qrr1
Biofilm
Motility

ABSTRACT

Colonization of the squid *Euprymna scolopes* by the bacterium *Vibrio fischeri* depends on bacterial biofilm formation, motility, and bioluminescence. Previous work has demonstrated an inhibitory role for the small RNA (sRNA) Qrr1 in quorum-induced bioluminescence of *V. fischeri*, but the contribution of the corresponding sRNA chaperone, Hfq, was not examined. We thus hypothesized that *V. fischeri* Hfq similarly functions to inhibit bacterial bioluminescence as well as regulate other key steps of symbiosis, including bacterial biofilm formation and motility. Surprisingly, deletion of *hfq* increased luminescence of *V. fischeri* beyond what was observed for the loss of *qrr1* sRNA. Epistasis experiments revealed that, while Hfq contributes to the Qrr1-dependent regulation of light production, it also functions independently of Qrr1 and its downstream target, LitR. This Hfq-dependent, Qrr1-independent regulation of bioluminescence is also independent of the major repressor of light production in *V. fischeri,* ArcA. We further determined that Hfq is required for full motility of *V. fischeri* in a mechanism that partially depends on the Qrr1/LitR regulators. Finally, Hfq also appears to function in the control of biofilm formation: loss of Hfq delayed the timing and diminished the extent of wrinkled colony development, but did not eliminate the production of SYP-polysaccharide-dependent cohesive colonies. Furthermore, loss of Hfq enhanced production of cellulose and resulted in increased Congo red binding. Together, these findings point to Hfq as an important regulator of multiple phenotypes relevant to symbiosis between *V. fischeri* and its squid host.

1. Introduction

The marine bacterium *Vibrio fischeri* exclusively colonizes the light organ of *Euprymna scolopes*, the Hawaiian bobtail squid (reviewed in (Norsworthy and Visick, 2013; Mandel and Dunn, 2016; Visick, 2009; Verma and Miyashiro, 2013; Visick et al., 2021). To establish a successful symbiosis with its host, *V. fischeri* needs to: 1) form an aggregate (a biofilm) on the surface of the symbiotic light organ; 2) disperse from the aggregate; 3) use chemotaxis and flagellar motility to enter the light organ and migrate into deep crypt spaces; 4) survive the physical and chemical aspects of the passage to the deep crypts; and 5) grow to high density and produce light in response to a quorum. Each aspect of this colonization process has been investigated and key regulatory and/or structural factors identified for each (reviewed in (Visick et al., 2021)). These include the cues that *V. fischeri* monitors, i.e., chitin and other nutrients, nitric oxide (NO), and autoinducer concentrations, and to which it responds appropriately by modulating flagella function, exopolysaccharide synthesis, and light production (Thompson et al., 2019; Septer et al., 2013).

The Hfq protein has been identified in many bacterial species as a chaperone of small non-coding RNAs (sRNAs) that post-transcriptionally control target mRNAs (Kavita et al., 2018; Soper et al., 2010). The majority of sRNAs are 50–200 nucleotides long and have limited and imperfect complementarity with either the 5′ or 3′ untranslated region (UTR) of the mRNA they control (Gottesman and Storz, 2011). Negative regulation of a target by sRNA occurs either by promoting degradation of the transcript through recruitment of RNAse or blocking access of the ribosomes to the initiation site (Ikeda et al., 2011; Prévost et al., 2011; Lalaouna et al., 2015). Alternatively, sRNAs can activate translation by facilitating access of the ribosomes through removal of the secondary

Abbreviations: A, absorbance (1 cm); bp, base pair(s); cDNA, DNA complementary to RNA; nt, nucleotide(s); ORF, open reading frame; RBS, ribosome binding site; RLU, relative light units.

* Corresponding author.
E-mail address: vanya.tepavcevic@wheaton.edu (J. Tepavčević).

https://doi.org/10.1016/j.gene.2021.146048
Received 18 September 2021; Accepted 26 October 2021
Available online 29 October 2021

structures that may sequester the ribosome-binding site. Hfq-dependent sRNAs rely on Hfq for their stability (and some for their expression) and typically act *in trans* on the target mRNAs. The chaperone binds to the AU-rich sequences of the mRNAs that it controls. A variety of genetic, biochemical and computational approaches have recently been employed to identify Hfq-associated sRNAs, as well as the large number of target mRNAs that they regulate (Hör et al., 2018; Han et al., 2016; King et al., 2019). Delineating the physiological role of the sRNA interactions with their targets and the contribution of Hfq to particular phenotypes have been more challenging. There is a need to dissect the pathways of post-transcriptional control of gene expression via these regulators to achieve a more comprehensive picture of the layers of regulation required by bacteria under numerous conditions.

By facilitating base-pairing interactions of sRNAs with mRNAs, Hfq has been previously reported to regulate biofilm formation, virulence and many other phenotypes (Bellows et al., 2012; Deng et al., 2016; Lenz et al., 2004; Liu et al., 2019; Schachterle Jeffrey et al., 2019). However, it appears that the role of Hfq is species specific and the inactivation of Hfq has resulted in a range of effects in different species. *hfq* deletion strains have exhibited impaired growth, difficulties in coping with environmental stresses, changes in susceptibility to antibiotics, and for organisms that are pathogens, decreased virulence (Bellows et al., 2012; Deng et al., 2016).

One characterized example of an sRNA with a role in regulation of the *V. fischeri*-squid symbiosis is Qrr1 (Miyashiro et al., 2010). This homolog of Qrr1-4 from *V. cholerae* and *V. harveyi* (Lenz et al., 2004; Tu and Bassler, 2007; Bardill et al., 2011; Zhao et al., 2013) post-transcriptionally represses LitR, a master regulator of the bioluminescence operon (*lux*) (Fidopiastis et al., 2002) (Fig. 1). Despite the reported function of Qrr1 in controlling luminescence, the exact contribution of the sRNA chaperone Hfq to this regulation and other aspects of the physiology of *V. fischeri* has not been examined. Given the importance of Hfq in other bacteria, we hypothesized that Hfq could supply additional (post-transcriptional) control over key steps of symbiosis between the marine bacterium and its squid host, including bioluminescence, motility, and biofilm formation (Fig. 1). Here, we find that Hfq not only plays a key role in each of these processes but also that it functions via both Qrr1-dependent and -independent mechanisms, indicating the contribution of an as-yet unknown sRNA regulator in well-described processes such as bioluminescence.

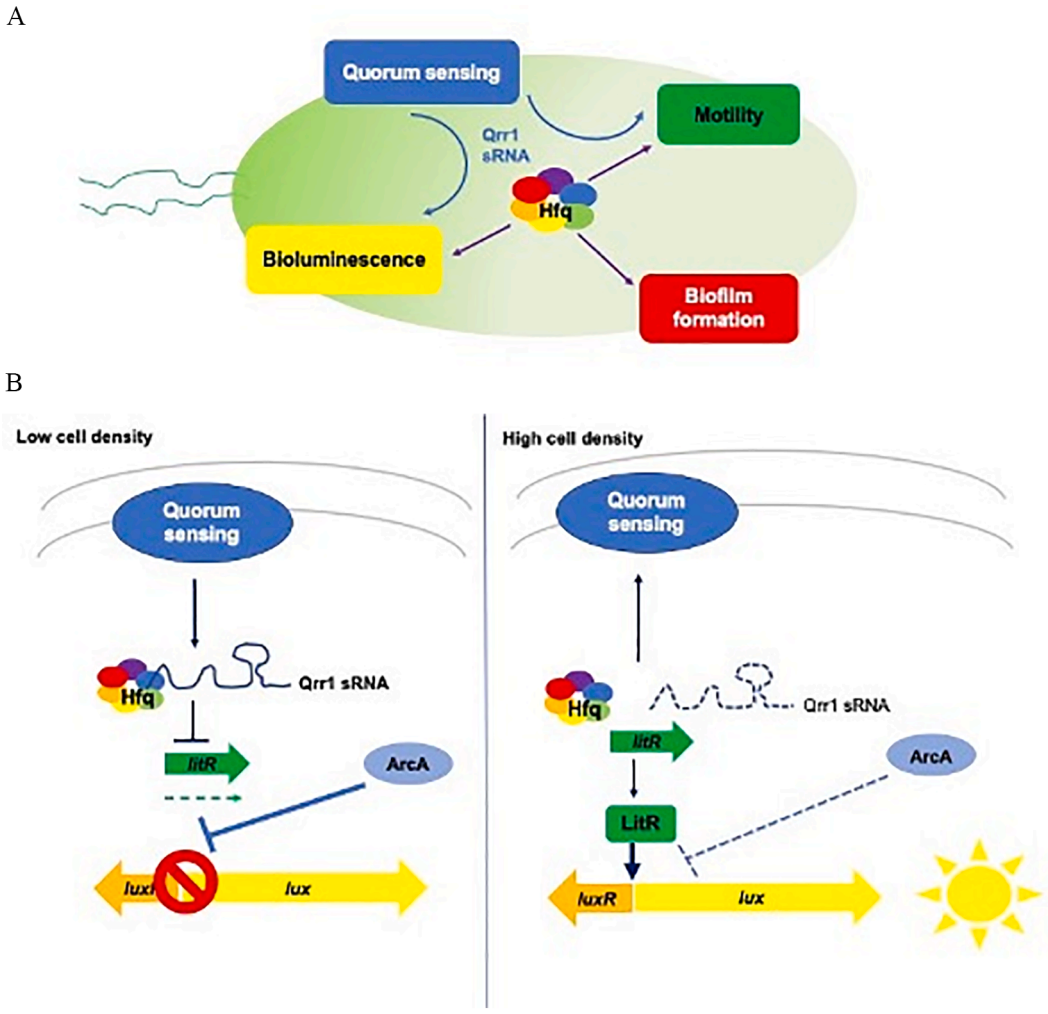

Fig. 1. Model for the role of Hfq in pathways important for host colonization by *V. fischeri*. A. Work presented here shows that Hfq works via both Qrr1-dependent (blue arrows) and -independent (purple arrows) mechanisms; a role for Qrr1 in controlling biofilm formation is unclear. B. Regulation of bioluminescence in *V. fischeri.* At low cell density (left panel) expression of sRNA Qrr1 is induced by the quorum sensing regulator LuxO (not shown). In turn, Qrr1 represses LitR at a post-transcriptional level, resulting in little to no light production. Independent of quorum sensing, luminescence is negatively regulated by transcriptional repressor ArcA. When *V. fischeri* cells reach quorum (right panel), the repression of *litR* expression is relieved due to a decrease in *qrr1* expression. At high cell density, LitR acts as the major positive regulator of bioluminescence by activating transcription of *luxR*, which encodes the direct transcriptional activator of the *lux* operon. The positioning of the Hfq chaperone in this diagram was based on models of its role in related organisms and has been supported by the genetic analyses in this work. (For interpretation of the references to color in this figure legend, the reader is referred to the web version of this article.)

2. Materials and methods

2.1. Strains and media

Bacterial strains used and generated in this study are listed in Table 1. *V. fischeri* strain ES114 (Boettcher and Ruby, 1990) was used as a genetic background for all further genetic manipulations. For routine culturing of *V. fischeri* strains, Luria-Bertani (LB) medium supplemented with sodium chloride and Tris (pH 7.5) (LBS) (Stabb et al., 2001) was used. Other media were used for phenotype analysis as described below. *E. coli* strains were cultured on LB (Davis et al., 1980) medium at 37 °C and supplemented with antibiotics and thymidine when needed. Antibiotics were added as appropriate at the following final concentrations: For *V. fischeri*: Chloramphenicol (Cm) 1 μg ml^{-1} for single copy selection or 5 μg ml^{-1} for plasmid maintenance, Erythromycin (5 μg ml^{-1}), Kanamycin (Kan) (100 μg ml^{-1}). For *E. coli*: Ampicillin (100 μg ml^{-1}), Chloramphenicol (Cm) (12.5 μg ml^{-1}), Kanamycin (Kan) (50 μg ml^{-1}) (Table 2).

2.2. Growth curves

Strains of *V. fischeri* were cultured overnight in LBS or TMM (Tris Minimal Medium, which contains 300 mM sodium chloride, 50 mM magnesium sulfate, 0.33 mM potassium phosphate dibasic, 10 μM ferrous ammonium sulfate, 0.1% ammonium chloride, 10 mM N-acetylglucosamine, 10 mM potassium chloride, 10 mM calcium chloride, and 100 mM Tris pH 7.5) at 28 °C for 14 h. The cultures were then diluted to OD_{600} of 0.1 in 30 ml of LBS medium or to OD_{600} of 0.05 in 30 ml of TMM medium in 250 ml baffled flasks and incubated at 28 °C or 24 °C with 220 rpm of consistent shaking. Aliquots were withdrawn every hour for ten hours and the optical densities were measured with BioMate 3 Thermo Spectronic. The experiments were performed in triplicate.

2.3. Strain construction/complementation

Mutant strains were generated by transformation using a previously described procedure (Christensen et al., 2020) with either genomic DNA (gDNA) from a marked mutant or PCR products (primer sequences listed in Table 3) generated via a PCR SOE approach (Visick et al., 2018). For the latter approach, sequences of about 500 bp from regions up- and downstream of the gene of interest were fused on either side of an antibiotic resistance cassette. Strains in which the composite fragment had recombined into the chromosome were selected using the appropriate antibiotic, and evaluated to confirm that gene replacement had occurred by PCR using the external primers. In some cases, intermediate strains were used as the initial recipient of the PCR DNA; from these strains, gDNA was collected and used to transform the appropriate final recipient.

2.4. Motility assay

Bacteria were cultured overnight at 28 °C in tryptone broth with added sodium chloride (TBS; contains 1% tryptone and 2% sodium chloride) (DeLoney-Marino et al., 2003). After ~ 2 h subculture in the same medium, the bacteria were standardized to an equal optical density at 600 nm (OD_{600}) between 0.2 and 0.3. Aliquots of 10 μl were spotted on TBS soft agar (0.25% agar) supplemented with 35 mM $MgSO_4$ and incubated at 28 °C. The outer diameter of swimming cultures was measured hourly for 6 h. In addition, photographs were taken at the indicated time.

2.5. Luminescence measurements

V. fischeri was cultured overnight in SWT (Sea Water Tryptone; contains 70% artificial sea water, 0.5% tryptone, 0.3% yeast extract)

Table 1
V. fischeri strains used in this study.

Strain	Genotype	Derivation[1]	Source/ Reference
AMJ2	Δ*arcA*	N/A	(Bose et al., 2007)
ES114	Wild Type	N/A	(Boettcher and Ruby, 1990)
JB19	*litR*::erm	N/A	(Bose et al., 2007)
JB21	Δ*arcA litR*::erm	N/A	(Bose et al., 2007)
KV7860	Δ*binK*	N/A	(Tischler et al., 2018)
KV7908	Δ*bcsA* Δ*binK*	N/A	(Tischler et al., 2018)
KV8408	*bcsA*::Tn*5*	N/A	(Visick et al., 2018)
KV8563	Δ*qrr*1 Δ*hfq*::FRT-erm	NT pLostfoX-Kan/TIM305 with pDNA, primers 2416 & 2417 (ES114), 2089 & 2090 (pKV494), and 2418 & 2419 (ES114)	This study
KV8573	IG (*yeiR-glmS*):: Erm^R-trunc $Trim^R$ Δ*hfq*::FRT-Cm	NT pLostfoX-Kan/KV8232 (61) with pDNA, primers 2416 & 2417 (ES114), 2089 & 2090 (pKV495), and 2418 & 2419 (ES114)	This study
KV8576	Δ*arcA* Δ*hfq*::FRT-Erm	NT pLostfoX-Kan/AMJ2 with pDNA, primers 2416 & 2417 (ES114), 2089 & 2090 (pKV494), and 2418 & 2419 (ES114)	This study
KV8577	Δ*arcA* Δ*qrr1*::FRT-Erm	NT pLostfoX-Kan/AMJ2 with pDNA, primers 2424 & 2425 (ES114), 2089 & 2090 (pKV494), and 2426 & 2427 (ES114)	This study
KV9050	Δ*hfq*::FRT-Cm	NT pLostfoX-Kan/ES114 with gKV8573	This study
KV9069	Δ*binK* Δ*hfq*::FRT-Cm	Transformation pLostfoX-Kan/ KV7860 with gKV8573	This study
KV9072	Δ*hfq*::FRT-Cm IG (*yeiR*-FRT-erm/ *glmS*)::*hfq*$^+$	NT pLostfoX-Kan/KV9050 with pDNA, primers 2290 & 2090 (pKV502), 2420 & 2421 (ES114) & 2196 & 1487 (pKV503)	This study
KV9075	Δ*binK* Δ*hfq*::FRT-Cm IG (*yeiR*-FRT-erm/*glmS*)::*hfq*$^+$	NT pLostfoX-Kan/KV9069 using pDNA, primers 2290 & 2090 (pKV502), 2420 & 2421 (ES114) & 2196 & 1487 (pKV503)	This study
KV9347	Δ*qrr*1 Δ*binK*::FRT-Trim	NT plostfoX/TIM305 with gKV8458 (6)	This study
KV9444	Δ*binK litR*::erm	NT pLostfoX-Kan/KV7860 with gJB19	This study
KV9445	Δ*bcsA* Δ*binK* Δ*hfq*:: FRT-Cm	NT pLostfoX-Kan/KV7908 with gKV9050	This study
TIM305	Δ*qrr1*	N/A	(Miyashiro et al., 2010)
VAW43	Δ*qrr1 litR*::erm	NT pLostfoX-Kan/TIM305 with gJB19	This study
VAW68	Δ*arcA* Δ*hfq*::FRT-Cm *litR*::erm	NT pLostfoX-Kan/KV8576 with gJB19	This study
VAW73	IG (*yeiR-glmS*):: Erm^R-trunc $Trim^R$ Δ*hfq*::FRT-Cm *litR*:: erm	NT pLostfoX-Kan/KV8573 with gJB19	This study
VAW74	Δ*arcA* Δ*hfq* Δ*litR*:: erm		This study
VAW75	Δ*qrr*1 Δ*hfq* Δ*litR*:: erm		This study

[1]NT, natural transformation; pDNA, DNA derived from PCR SOE reactions; g, genomic DNA of the indicated strain.

Table 2
Plasmids used in this study.

Plasmid	Description	Source/Reference
pKV494	pJET + FRT-Erm	(Visick et al., 2018)
pKV495	pJET + FRT-Cm	(Visick et al., 2018)
pKV502	pJET + yeiR-Erm	(Visick et al., 2018)
pKV503	pJET + glmS	(Visick et al., 2018)
plostfoX-Kan	pEVS79-Kan + tfoX	(Brooks et al., 2014)

medium at 28 °C. The cultures were then diluted to OD_{600} of 0.005 in 30 ml of SWTO (70% artificial sea water, 0.5% tryptone, 0.3% yeast extract, 2% sodium chloride) medium in 250 ml baffled flasks and incubated with shaking at 24 °C. Aliquots of 1 ml were withdrawn every hour and luminescence measured in Turner Biosystems Luminometer (Model TD-20/20) after aeration, followed by optical density (OD_{600}) reading with the BioPhotometer. Specific luminescence was determined as relative luminescence divided by OD_{600}. These values were plotted against the OD_{600} values to permit a comparison of luminescence levels at similar cell densities.

2.6. Wrinkled colony assay

Cultures grown in LBS overnight at 28 °C were sub-cultured 1:100 in LBS and incubated at 28 °C for 1.5 h. Density was standardized to OD_{600} 0.2 and 10 μl aliquots of culture were spotted on one-day old LBS agar plates with or without 10 mM $CaCl_2$. Wrinkling at 28 °C was monitored at the indicated times. At the last time point, the spots were disrupted to assess stickiness. Images of wrinkled colonies were generated using Zeiss Stemi 2000-c microscope and Jenoptik Gryphax Subra camera.

2.7. Congo red assay

For a liter of LBS agar, 40 mg congo red and 15 mg Coomassie blue were added to make LBS Congo Red agar plates two days prior to streaking. *V. fischeri* strains were streaked onto LBS agar plates and allowed to grow overnight. Heavy streaks were applied from the overnight plates onto LBS Congo Red agar plates. The streaks were transferred onto paper after incubation at 24 °C for 24 h to permit better visualization of the colony color, as described in (Tischler et al., 2018). To quantify the amount of red color produced by each strain, *V. fischeri* strains were grown overnight in LBS. The next day, the strains were subcultured 1:100. After 1.5 h of growth, all strains were normalized to an OD_{600} of 0.2 and spotted onto two-day old Congo red plates. Spots were transferred onto paper following incubation at 24 °C for 24 h. Color produced by each strain, denoted as the area, was quantified from scanned images using ImageJ.

2.8. qRT-PCR analysis

To isolate RNA for *litR* transcript analysis, cultures were grown in SWTO at 24 °C and aliquots collected at designated time points. Samples were mixed with 2x volume of RNA Protect Bacteria Reagent (Qiagen) and pellets stored after 10 min centrifugation at 5,000xg. RNA was extracted using MasterPure RNA purification kit (Epicentre) and treated with DNase to remove any genomic DNA. cDNA synthesis was performed using iScript kit (Bio-Rad) followed by qPCR using iTaq Universal SYBR Green Supermix (Bio-Rad) on the CFX9q Real-Time System instrument (Bio-Rad). Primers qlitR-F and qlitR-R were used to amplify *litR* (test) transcript. 5S rRNA-specific primers P2242 and P2243 were used to amplify the reference transcript. Fold change in *litR* mRNA levels was determined using $\Delta\Delta C_t$ method (Livak and Schmittgen, 2001).

2.9. Bioinformatic analysis

Amino acid sequences of the Hfq protein from *E. coli, V. fischeri, V. cholerae* and *V. harveyi* were retrieved from the NCBI database. The NCBI accession numbers used are as follows: 332,341,332 (*E. coli)*, 171,902,228 (*V. fischeri),* 229,368,777 (*V. cholerae)*, 57,822,740 (*V. harveyi)*. The alignment was performed using the multiple alignment (EMBL-EBI; (Sievers et al., 2011; Madeira et al., 2019). The phylogenetic tree of Hfq sequences was constructed using Phylogeny.fr (Dereeper et al., 2008).

2.10. Statistical analysis

GraphPad Prism (version 8) was used for graphical representation of results. Means and standard deviations were determined using the embedded statistics tools.

3. Results

3.1. 1 V. fischeri encodes a putative Hfq protein

The sequence of the putative Hfq protein from *V. fischeri* strain ES114 (encoded by *VF_2323*) was aligned with those from *E. coli*, *V. harveyi* and *V. cholerae* using the EMBOSS tool for multiple sequence alignment Clustal Omega (Fig. 2A) (Sievers et al., 2011). The N-terminal sequence of each of the four proteins is well conserved while the C-termini of the

Table 3
Oligonucleotides used in this study.

Primer	Purpose	Sequence[1]
2089	Amplify AbR cassette, F	CCATACTTAGTGCGGCCGCCTA
2090	Amplify AbR cassette, R	CCATGGCCTTCTAGGCCTATCC
2416	Delete hfq, upstream	CGTTGGAAGTATTTCGAATTTCG
2417	Delete hfq, upstream	taggcggccgcactaagtatggGCTATGAGCCTTTAGCTTATGAC
2418	Delete hfq, downstream	ggataggcctagaaggccatggCTAGAATAGTTAATCAGTTAAGG
2419	Delete hfq, downstream	GCTTTAATACGTTCACGCAACAATCG
2420	Complement hfq	ggataggcctagaaggccatggGCTTCAATGTTGTTTAACTTAAGTGC
2421	Complement hfq	taggcggccgcactaagtatggCCTTAACTGATTAACTATTCTAG
2290	Amplify from middle of ErmR	AAGAAACCGATACCGTTTACG
1487	Amplify glmS	GGTCGTGGGGAGTTTTATCC
2196	Amplify glmS	tCCATACTTAGTGCGGCCGCCTA
2424	Delete qrr1, upstream	GGTATCTTTTGGATTCTCTTGG
2425	Delete qrr1, upstream	taggcggccgcactaagtatggCCTATTGCAGGGAGCGTGCCAAC
2426	Delete qrr1, downstream	ggataggcctagaaggccatggGCTATAAAATCAATAACTAACTATTC
2427	Delete qrr1, downstream	CGCTTAGGTGAGTTTGATGTCC
2242	5S rRNA, qRT-PCR, F	TGATCCCATGCCGAACTCAGAAG
2243	5S rRNA, qRT-PCR, R	CCTGGCGATGTCCTACTCTCAC
qlitR-F	litR, qRT-PCR, F	AAGGCCTAGAACAAGGCTATC
qlitR-R	litR, qRT-PCR, R	GACAGAGACCTGAGCGATTT

[1]Lowercase letters indicate "tail" sequences not complementary to the template.

Vibrio proteins lack 13 amino acids found in the *E. coli* Hfq protein. Of the 72 N-terminal amino acids in *Vibrio* Hfq protein sequences, 69 are identical to those of *E. coli*, while only 6% of the C-terminal residues have homology to the *E. coli* Hfq. The phylogenetic tree (Dereeper et al., 2008) (Fig. 2B) constructed using the Hfq sequences of the four species reflects the 93.3% identity between the *V. fischeri* and *V. harveyi* proteins and 91% identity between *V. fischeri* and *V. cholerae*. This high level of conservation between the members of the *Vibrionaceae* family is expected and has been reported previously (Vincent et al., 2012). The *V. fischeri* protein is overall 68.3% identical to the *E. coli* sequence, indicating the lesser homology of the overall sequence between different gamma-proteobacteria, mostly due to the difference in length and content of the C-terminal tail. Given the conservation of the *V. fischeri* protein and our phenotypic characterization described below, we designate *VF_2323* as *hfq*.

3.2. Hfq is required for growth of V. fischeri in minimal medium

In other bacteria (including *E. coli*), Hfq controls a variety of traits including bacterial growth (Tsui et al., 1994; Christiansen et al., 2004; Robertson and Roop, 1999; Arce-Rodríguez et al., 2016; Bai et al., 2010). To begin to understand the function of Hfq in *V. fischeri*, we generated *hfq* deletion and complementation strains. When grown at the optimal growth temperature of 28 °C in a complex medium, these strains displayed no substantial differences in growth rates or final growth yields (Fig. 3A). Thus, loss of *hfq* does not affect growth of *V. fischeri* under these conditions. Similarly, when cultured in a complex medium at 24 °C, there were no differences in growth of the three strains (Fig. 3B). In contrast, when grown in a minimal medium, the *hfq* mutant exhibited a severe defect in growth, especially at 24 °C (Fig. 3C, D). Supplementing the medium with casamino acids restored growth to wild type levels (Fig. 3D). This suggests that Hfq serves as a pleiotropic regulator of gene expression in *V. fischeri*, required for optimal growth under nutrient-limiting conditions.

3.3. Hfq regulates luminescence in V. fischeri

In other *Vibrio* species such as *V. cholerae*, Hfq functions in the quorum sensing pathway to negatively control production of the key regulator HapR at low cell density (Deng et al., 2016). In *V. fischeri*, Hfq is predicted to similarly control the HapR homolog LitR, which in turn controls luminescence (Fig. 1) (Miyashiro et al., 2010). To test this prediction, we evaluated luminescence of the *hfq* mutant (Fig. 4). Consistent with the predicted negative regulatory function of Hfq, we found that the specific luminescence in the Δ*hfq* strain, represented as relative luminescence per OD_{600}, was increased 100-fold as compared to the wild-type strain, and this phenotype was complemented by restoring *hfq* to the mutant strain (Fig. 4). This altered light production was not due to a defect in growth, as growth of the *hfq* mutant was indistinguishable from that of the wild-type parent under the conditions used for this assay (Supp. Fig. 1).

3.4. Hfq function overlaps with but is distinct from Qrr1 in controlling luminescence

In *V. harveyi*, Hfq functions with any of five related sRNAs (Qrr1-5) to control LuxR production and quorum-dependent phenotypes, while in *V. cholerae* four Hfq-dependent sRNAs (Qrr1-4) regulate expression of transcription factor HapR (Lenz et al., 2004; Tu and Bassler, 2007; Bardill et al., 2011). In contrast, *V. fischeri* contains only a single gene for Qrr, *qrr1* (Miyashiro et al., 2010). A *qrr1* deletion mutant was previously reported to exhibit increased luminescence (Miyashiro et al., 2010); however, only the maximal luminescence of the *qrr1* mutant was reported (Miyashiro et al., 2010), and no studies of *hfq* were included. Given that *V. fischeri* contains a single *qrr1* gene, we predicted that the luminescence phenotypes of the *hfq* and *qrr1* mutants would be the same. To test this prediction, we evaluated the relative luminescence levels of Δ*qrr1* and Δ*hfq* mutants. As previously observed, the *qrr1* mutant produced increased luminescence compared to the wild-type strain (Miyashiro et al., 2010; Lyell et al., 2013) (Fig. 5). Unexpectedly, however, the Δ*hfq* strain was ten-fold more luminescent than the *qrr1* mutant at the peak of luminescence (Fig. 5). These data demonstrate that Hfq is indeed a repressor of luminescence in *V. fischeri* and suggest that Hfq has a function(s) in controlling luminescence that is independent of Qrr1.

To further understand the relationship between Hfq, Qrr1 and

A.

```
E. coli     MAKGQSLQDPFLNALRRERVPVSIYLVNGIKLQGQIESFDQFVILLKNTVSQMVYKHAISTVVPSRPVSHHSNNAGGGTSSNYHHGSSAQNTSAQQDSEETE 102
V. fischeri MAKGQSLQDPFLNALRRERIPVSIYLVNGIKLQGQIESFDQFVILLKNTVNQMVYKHAISTVVPARAVSHHSASDRPQGER-------PQ-----EKTEE-- 88
V. harveyi  MAKGQSLQDPFLNALRRERIPVSIYLVNGIKLQGQIESFDQFVILLKNTVNQMVYKHAISTVVPARPVSHHS-GDRPQGDR-------PQ-----EKSED-- 87
V. cholerae MAKGQSLQDPFLNALRRERIPVSIYLVNGIKLQGQIESFDQFVILLKNTVNQMVYKHAISTVVPARPVSHHS-GARPASDR-------PA-----EKSEE-- 87
            ********************:******************************.*************:* ***** .   .              :.:*:
```

B.

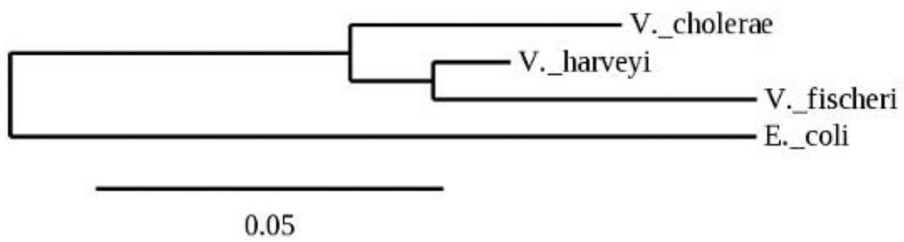

Fig. 2. Comparison of Hfq sequences from *E. coli*, *V. fischeri*, *V. harveyi* and *V. cholerae*. A. Protein sequence alignment using EMBOSS Clustal Omega (Sievers et al., 2011) Asterisks indicate identical amino acid residues, dashes indicate absence of residues, single and double dots indicate amino acid substitutions. B. Phylogenetic tree of Hfq sequences was generated using Phylogeny.fr (Dereeper et al., 2008) and rooted with the *E. coli* Hfq sequence.

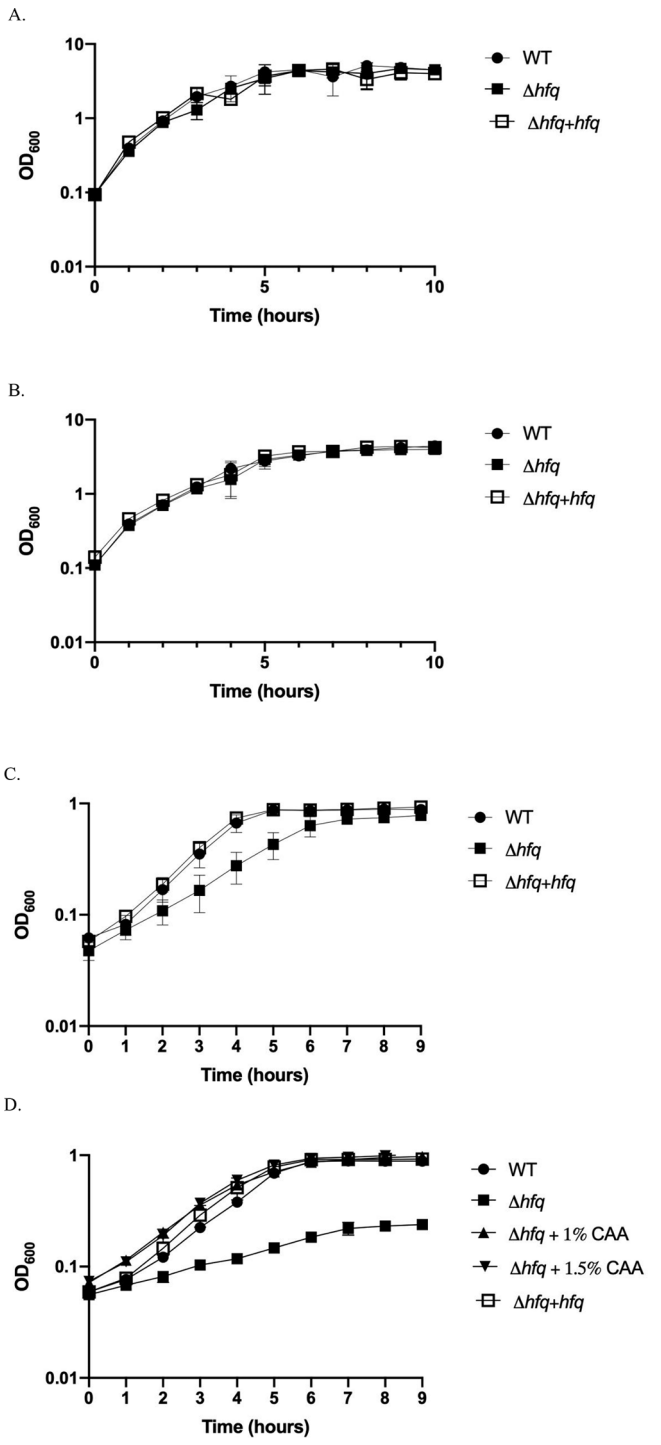

Fig. 3. Deletion of *hfq* affects growth of *V. fischeri* in minimal, but not complex, medium. Wild-type (WT) ES114 (black circles), Δ*hfq* (KV9050, black squares) and complemented Δ*hfq* + *hfq* (KV9072, open squares) strains were cultured in LBS medium at 28 °C (A) and 24 °C (B) and cell density measurements were taken hourly. The same strains were grown in TMM at 28 °C (C) and 24 °C (D). The Δ*hfq* strain was also cultured in TMM at 24 °C in the presence of 1% (up triangles) and 1.5% (down triangles) casamino acids (CAA) (D). All data are represented as means and standard deviation of triplicate biological replicates. Experiments were repeated on at least three independent occasions.

control of luminescence, we generated a double *hfq qrr1* mutant. This strain phenocopied the Δ*hfq* single mutant with levels of luminescence that were ten-fold greater than the strain that only lacks Qrr1 (Fig. 5). These data reveal that Hfq is dominant to Qrr1 in the bioluminescence pathway and support the hypothesis that Hfq has a function independent of Qrr1.

3.5. Hfq functions independently of LitR to control luminescence

Our data indicated that Hfq represses luminescence independently of Qrr1. Because Qrr1 targets LitR translation (Miyashiro et al., 2010; Miyashiro and Ruby, 2012), we hypothesized that Hfq could function with an additional sRNA to control LitR translation and thus luminescence. Alternatively, Hfq could control luminescence at a distinct point in the luminescence pathway (Fig. 1). To distinguish between these possibilities, we compared the luminescence phenotypes of single and double mutants of *hfq*, *qrr1*, and *litR*. As previously reported, the *litR* mutant produced low levels of luminescence, while the single *hfq* and *qrr1* mutants exhibited increased luminescence as described above (Fig. 6) (Miyashiro and Ruby, 2012; Kimbrough et al., 2016). The double *qrr1 litR* mutant produced minimal amounts of light similar to the *litR* single mutant (Fig. 6) as expected given the direct role of Qrr1 in controlling LitR production (Miyashiro et al., 2010). In contrast, however, the double *hfq litR* mutant achieved increased levels of light relative to the *litR* mutant, although diminished relative to the wild-type and *hfq* single mutant strains. These data confirm the conclusion that Hfq has a role independent of Qrr1 and indicate that this effect occurs at a level distinct from control of LitR.

To assess whether Hfq cooperates with Qrr1 in controlling levels of LitR, we measured *litR* transcript levels in strains lacking *hfq* and *qrr1*. As previously reported (Miyashiro et al., 2010), the levels of *litR* transcript were increased in the Δ*qrr1* strain as compared to wild- type, but only at an early time point, two hours after subculture (Fig. 7). After this time point, the levels of *litR* mRNA returned to approximately wild-type levels. In the *hfq* mutant strain, *litR* expression was increased for at least an additional hour (Fig. 7) and then returned to the levels comparable to that of wild-type and the *qrr1* mutant strain. The different *litR* mRNA levels in the two strains suggest that Hfq and Qrr1 may control *litR* in concert for a short period of time after which Hfq regulation may continue without Qrr1. This subtle distinction in regulation of *litR* by the chaperone and the sRNA is additional support that Hfq can contribute to bioluminescence control with room for additional targets.

3.6. Hfq exerts its function independent of negative regulator ArcA

Another major regulator of luminescence is the response regulator ArcA, which binds to the promoter region upstream of *luxI* to inhibit luminescence (Fig. 1B) (Bose et al., 2007; Septer et al., 2012; Lyell et al., 2010). Thus, we considered the possibility that Hfq could inhibit light production independently of Qrr1 and LitR by controlling ArcA production or activity. If that were the case, then the quorum sensing-independent effect of Hfq on luminescence would depend on ArcA. To test this possibility, we examined light production of strains with single or multiple mutations (Fig. 8A). As reported previously, loss of the major repressor of luminescence ArcA led to increased light production (Bose et al., 2007), even at low cell density. This light phenotype was distinct from and higher than that of the Δ*hfq* Δ*qrr1* mutant (Fig. 8A), suggesting that ArcA is more potent at repressing luminescence than Hfq. Loss of both ArcA and Qrr1 resulted in higher light production than the ArcA single mutant. This result is consistent with the fact that these regulators exert effects at different points in the luminescence pathway (Fig. 1B). When both *arcA* and *hfq* were deleted, the resulting strain produced levels of light that were higher not only than the *arcA* single mutant but also the *arcA qrr1* double mutant; the difference between these two double mutants is similar to that seen for the single *hfq* and *qrr1* mutants (Fig. 8A). Furthermore, a triple mutant lacking all three negative regulators exhibited levels of light indistinguishable from the *arcA hfq* double mutant. These data suggest that Hfq exerts its function independently of ArcA activity.

Because the three regulators exert effects in the same direction, we

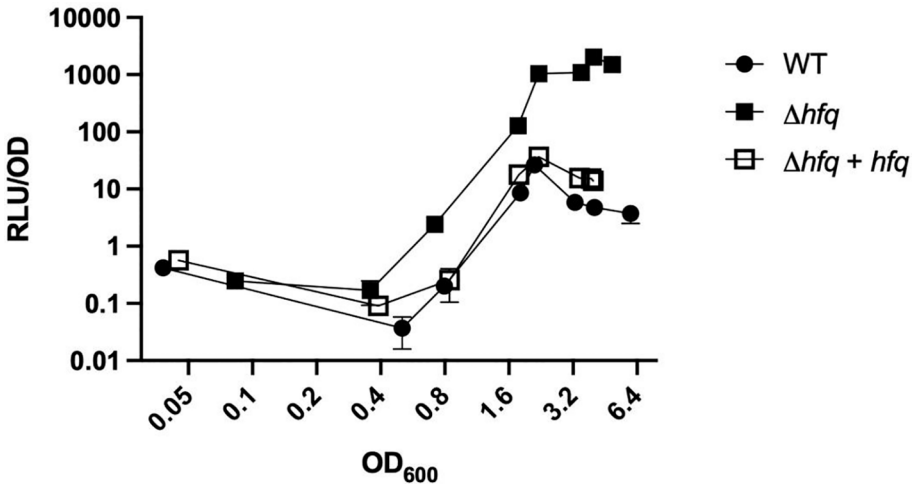

Fig. 4. Hfq is a repressor of bioluminescence. Luminescence levels of the Wild-type (WT) (ES114, black circles), Δ*hfq* mutant (KV9050, black squares), and complemented mutant Δ*hfq* + *hfq* (KV9072, open squares) strains were monitored over time during growth in SWTO at 24 °C. Relative light production (RLU) was averaged between duplicate measurements, normalized to cell density, and plotted against the optical density of the culture as described in the Materials and Methods section. The graph is a representative of at least three independent experiments performed in duplicate and the error bars represent SD.

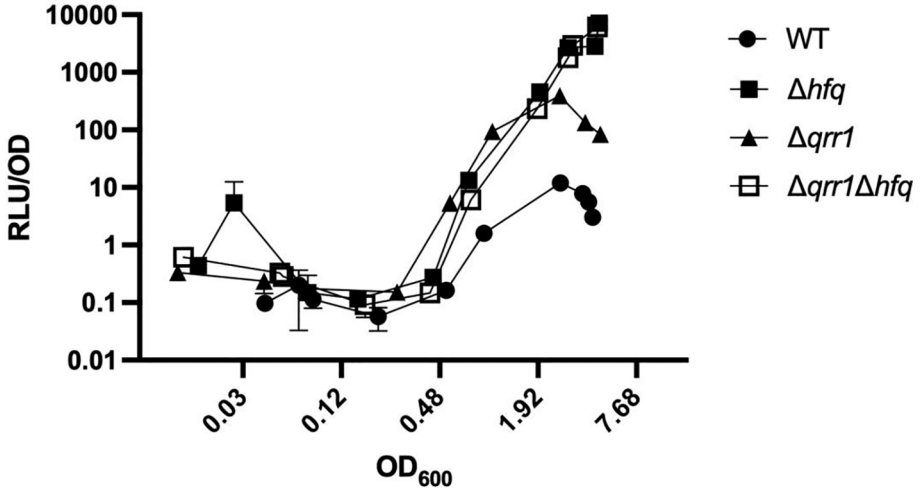

Fig. 5. Hfq and Qrr1 both repress luminescence, with Hfq having roles independent of Qrr1. Bioluminescence assay measuring light production by the Wild-type (WT) (ES114, black circles) and strains lacking either *hfq* (KV8573, black squares), *qrr1* (TIM305, up triangles) or both the chaperone and the sRNA (KV8563, open squares). A representative experiment done in triplicate is shown.

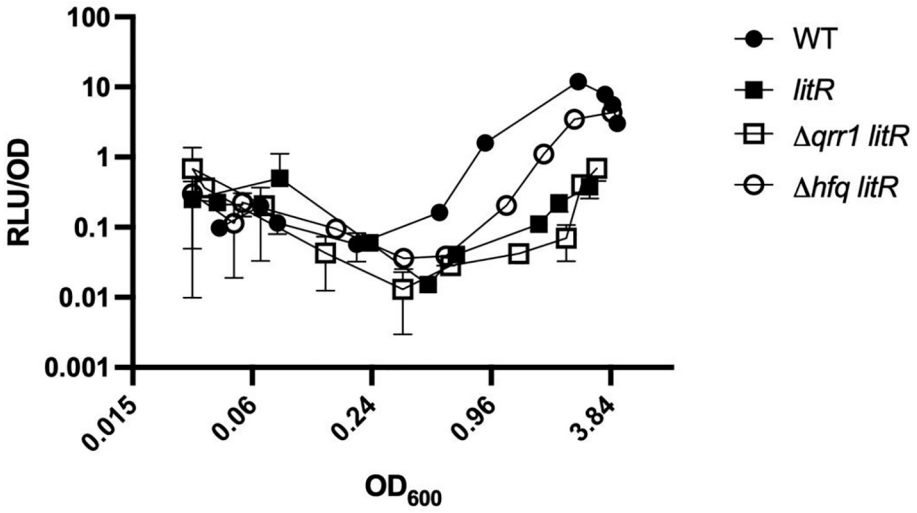

Fig. 6. Hfq and LitR independently control a converging target in the luminescence pathway. Luminescence levels of the Wild-type (WT) (ES114, black circles), *litR* (JB19, black squares), Δ*qrr1 litR* (VAW43, open squares) and Δ*hfq litR* (VAW73, open circles) strains were monitored over time during growth in SWTO at 24 °C. Relative light production (RLU) was measured in duplicate, normalized to cell density, and plotted against the optical density of the culture as described in the Materials and Methods section. The graph is a representative of at least three independent experiments performed in duplicate and the error bars represent SD.

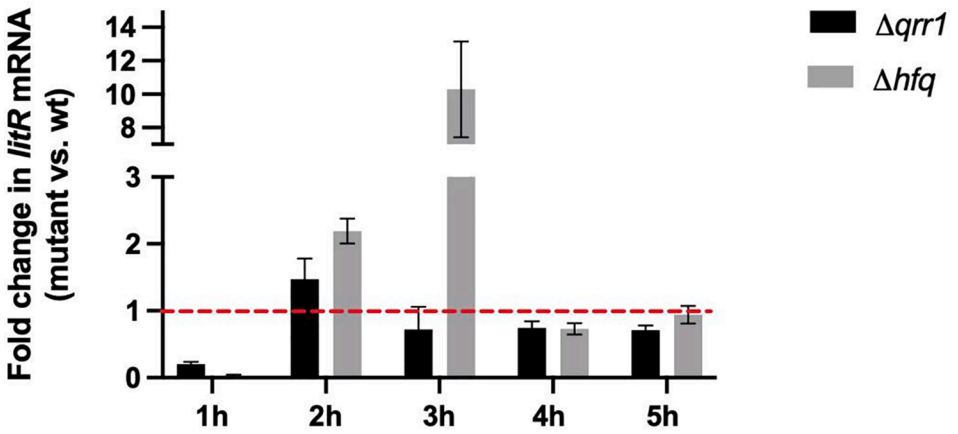

Fig. 7. Hfq effect on *litR* expression is distinct from the effect of Qrr1. *litR* transcript levels in strains lacking either *hfq* (KV8573) or *qrr1* (TIM305) were measured by quantitative RT-PCR and compared to the Wild-type (WT) (ES114) at different time points. Red dashed line represents the level of *litR* transcript in the WT *V. fischeri.* Error bars indicate SD of triplicate measurements. The graph is a representative of two independent experiments.

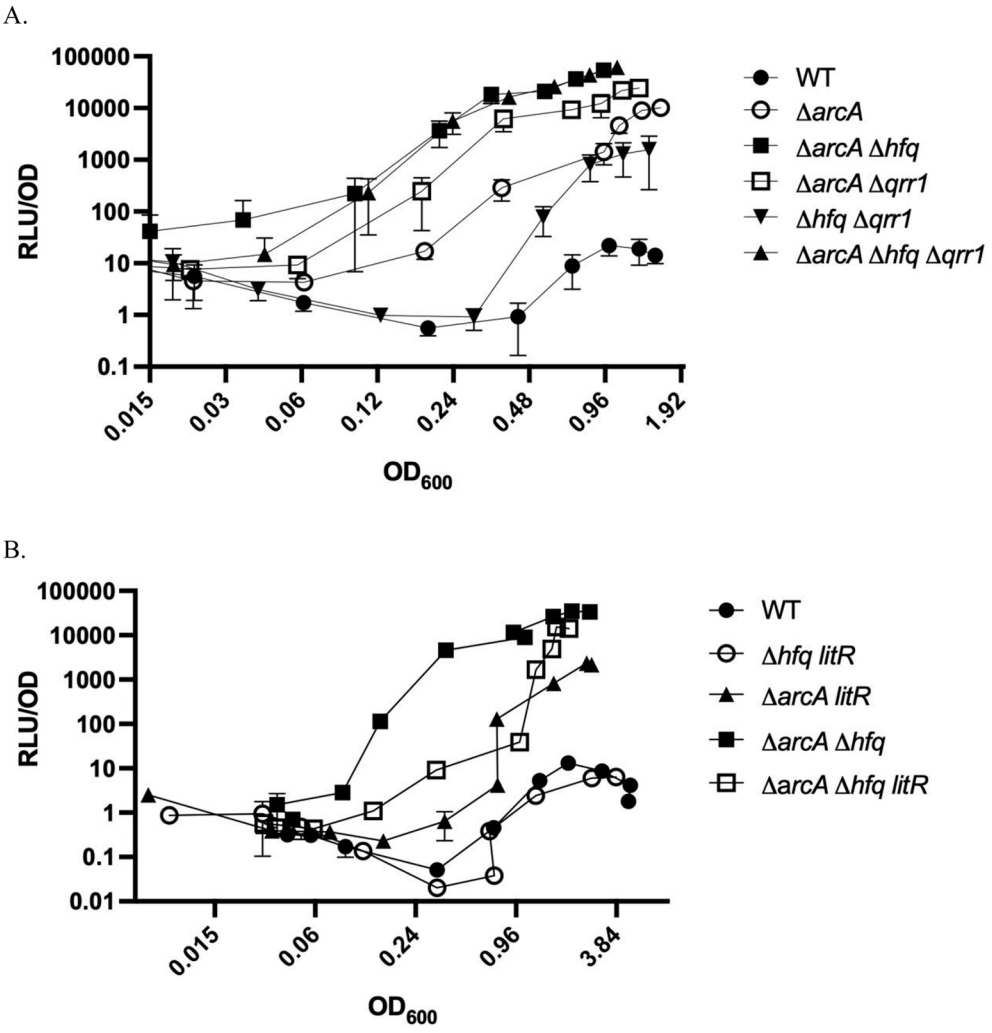

Fig. 8. Epistatic analysis of the role of Hfq, Qrr1, LitR and ArcA in controlling *V. fischeri* bioluminescence. A. Hfq and Qrr1 augment the repression of luminescence by ArcA. Luminescence levels of the Wild-type (WT) (ES114, black circles), Δ*arcA* (AMJ2, open circles) Δ*arcA* Δ*hfq* (KV8576, black squares), Δ*arcA* Δ*qrr1* (KV8577, open squares), Δ*hfq* Δ*qrr1* (KV8563, down triangles) and Δ*arcA* Δ*hfq* Δ*qrr1* (VAW68, up triangles) strains were monitored over time during growth in SWTO at 24 °C. Relative light production (RLU) was measured in duplicate, normalized to cell density, and plotted against the optical density of the culture as described in the Materials and Methods section. B. Hfq controls luminescence through a LitR- and ArcA-independent mechanism(s). Luminescence levels of the Wild-type (WT) (ES114, black circles), Δ*arcA* Δ*hfq* (KV8576, black squares), Δ*arcA litR* (JB21, triangles), Δ*arcA* Δ*hfq litR* (VAW74, open squares) and Δ*hfq litR* (VAW73, open circles) strains were monitored as above. Each of the graphs is a representative of at least three independent experiments performed in duplicate and the error bars represent SD.

performed one more set of epistasis experiments to solidify our understanding of the role of Hfq relative to the other regulators. Specifically, because Qrr1 functions upstream of LitR, and because disruption of *litR* exerts the opposite phenotype (decreased rather than increased luminescence), we assessed the luminescence properties of the *arcA hfq litR* triple mutant relative to the double mutants. Similar to what we observed for the *arcA hfq qrr1* triple (Fig. 8A) the *arcA hfq litR* triple exhibited increased luminescence relative to the *arcA litR* double mutant (as well as the *hfq litR* mutant), but less than the *arcA hfq* double (Fig. 8B). Together, these data indicate Hfq functions to control luminescence through both a Qrr1- and LitR-dependent mechanism and a mechanism that is independent of those regulators and ArcA.

3.7. Hfq function overlaps with but is distinct from Qrr1 in controlling motility

LitR is known to control *V. fischeri* motility (Lupp and Ruby, 2005). Thus, we wondered if Hfq would also control motility, and if so, if that control occurs exclusively via the effect of Hfq on the pathway that involves the quorum sensing regulators Qrr1 and LitR. To test this possibility, we first examined the effect of the loss of Hfq on motility of *V. fischeri* in a soft agar medium. Motility was decreased in the Δ*hfq* strain compared to the wild-type strain (Fig. 9). This defect was restored by complementation with *hfq*. Thus, Hfq is a positive regulator of motility in *V. fischeri*.

Given that Hfq functions both with and independently of Qrr1 to control luminescence, we wondered if the role of Hfq in controlling motility was dependent on or independent of Qrr1. We thus evaluated motility of strains that lacked either the chaperone or the sRNA or both. We observed a modest defect in motility for a *qrr1* single mutant, as has been reported previously (Fig. 10A). The single *hfq* mutant had a more severe motility defect than the *qrr1* mutant. Finally, the double mutant phenocopied the *hfq* mutant. Together, these data suggest that control of motility by Hfq is distinct from control by Qrr1.

Because both mutations caused decreased motility, however, it was not possible to fully assess the epistatic relationship between these regulators. To ask this question, we evaluated mutants that also lacked LitR. Although disruption of *litR* has been reported to increase motility (Lupp and Ruby, 2005), under our conditions, the *litR* mutant exhibited motility that was similar to the wild-type parent (Fig. 10B). The double *litR qrr1* mutant strain also phenocopied the wild-type strain. This result indicates that the *litR* mutation suppressed the motility defect of the *qrr1* mutant, supporting previous findings of increased motility for a *litR*

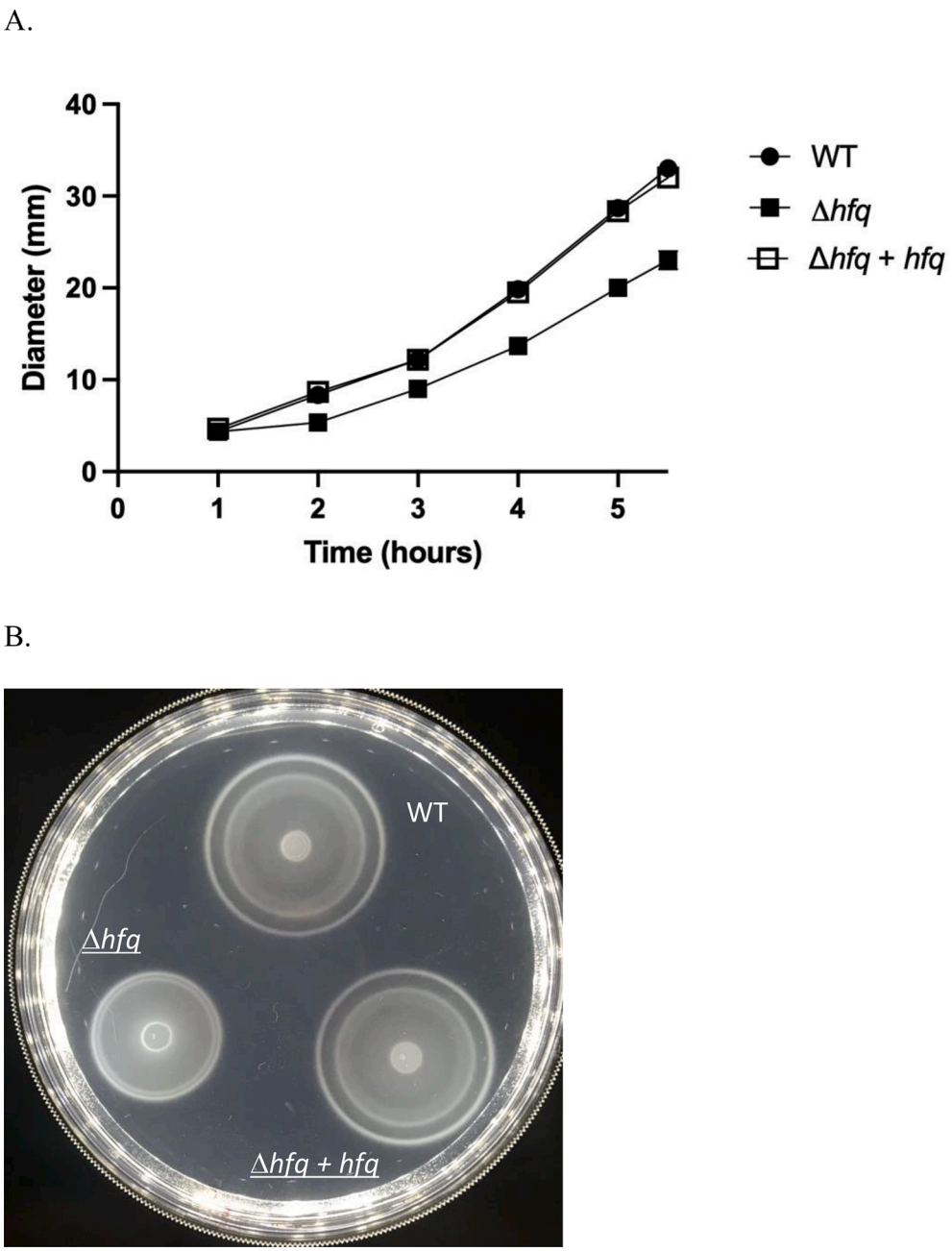

Fig. 9. Loss of Hfq reduces *V. fischeri* motility. A. Migration of the Wild-type (WT) (ES114, black circles), Δ*hfq* mutant (KV9050, black squares), and complemented mutant Δ*hfq* + *hfq* (KV9072, open squares) strains was measured in TBS + Mg^{2+} agar (0.25%) over 5.5 h at 28 °C. A representative experiment done in triplicate is shown. Error bars correspond to SD. B. Representative image of a motility agar plate at the 5.5 h time point.

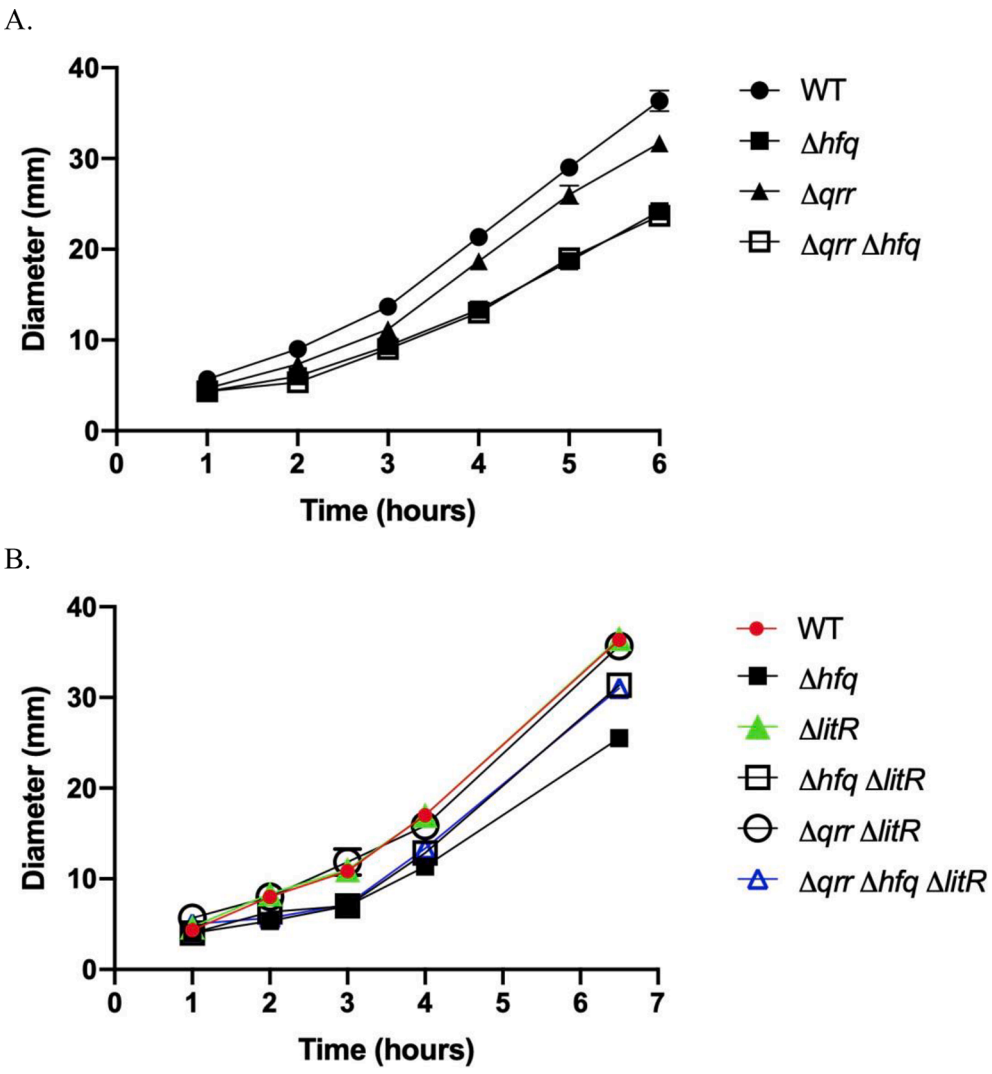

Fig. 10. Hfq promotes motility through a mechanism that is partially independent of LitR. A. Migration was examined in Wild-type (WT) (ES114, black circles), Δ*hfq* (KV8573, black squares), Δ*qrr1* (TIM305, triangles) and Δ*hfq* Δ*qrr1* (KV8563, open squares) strains as described in the legend to Fig. 9. A representative experiment done in triplicate is shown. Error bars correspond to SD. B. Strain lacking a repressor of motility (LitR) and either Hfq, Qrr1, or both were examined for motility. Wild-type (WT) (ES114, red circles), Δ*hfq* (KV8573, black squares), *litR* (JB19, green triangles), Δ*qrr1* *litR* (VAW43, open circles), Δ*hfq* *litR* (VAW73, open squares), and Δ*hfq* Δ*qrr1* *litR* (VAW75, open blue triangles). A representative experiment done in triplicate is shown. Error bars correspond to SD. (For interpretation of the references to color in this figure legend, the reader is referred to the web version of this article.)

mutant. In contrast, while the *litR hfq* mutant also had greater motility relative to the *hfq* mutant, it was not equivalent to the wild-type strain. Finally, the *litR hfq qrr1* triple mutant phenocopied the *litR hfq* double mutant. These data support the conclusion that Hfq stimulates motility through both Qrr1-dependent (LitR-dependent) and –independent mechanisms. Whether the Qrr1-independent control of motility by Hfq relies on the same downstream target/process as does the control of luminescence remains to be determined.

3.8. *Hfq is required for timely biofilm formation in V. fischeri*

Hfq has been found to control biofilm formation in other bacteria (Liu et al., 2019; Yao et al., 2018; Parker et al., 2017), which prompted us to ask if Hfq plays a similar role in *V. fischeri*. To answer this question, we used the wrinkled colony assay with a parent strain that lacks the negative regulator of biofilms, BinK (Brooks et al., 2016). While the parent strain started to form a biofilm at 24 h, as evidenced by visible colony architecture, the Δ*hfq* strain exhibited substantial, ~2-day delay in this process (Fig. 11A). Even at the last time point (72 h), the architecture of the wrinkled colony formed by the *hfq* mutant was distinct from its parent, *i.e.* less wrinkling by the mutant. However, at the final time point, the colony displayed a cohesiveness similar to that of its parent, indicating that SYP, the major polysaccharide responsible for colony cohesiveness (Ray et al., 2012), was sufficiently produced. The complemented *hfq* mutant was restored to the parental timing and pattern. This suggests that Hfq positively regulates biofilm formation in *V. fischeri*.

In the related microbe *Aliivibrio salmonicida*, LitR is a negative regulator of biofilm formation (Bjelland et al., 2012; Hansen et al., 2014). To date, no role in biofilm formation in *V. fischeri* has been reported for this regulator or for Qrr1. Because we found that Hfq acts both in concert with LitR and Qrr1 and in pathways independent of these regulators when controlling bioluminescence and motility, we explored whether Hfq regulates biofilm formation with the involvement of LitR and Qrr1. Under our conditions, which includes calcium to induce biofilm formation (Tischler et al., 2018), the Δ*qrr1* and *litR* strains show more, though subtle, wrinkling at earlier time points than the parent strain (compare time points 30 h, 36 h, and 48 h for the mutants vs. the parent Δ*binK* strain) (Fig. 11A). This increased biofilm phenotype implicates LitR and Qrr1 as repressors of biofilm formation, with LitR exerting a greater effect. In contrast to the other LitR and Qrr1-controlled phenotypes, however, biofilm formation is impacted in the same direction by both the Δ*qrr1* and *litR* mutations, rather than in opposite directions as would be expected. Furthermore, neither mutation exerts an effect in the same direction as the *hfq* mutant, making it unlikely that Hfq functions via these regulators to control biofilm formation. Overall, these results demonstrate that Hfq plays a key and previously unknown role in promoting wrinkled colony formation independent of the function of LitR and Qrr1, while also revealing roles for the latter regulators as biofilm inhibitors.

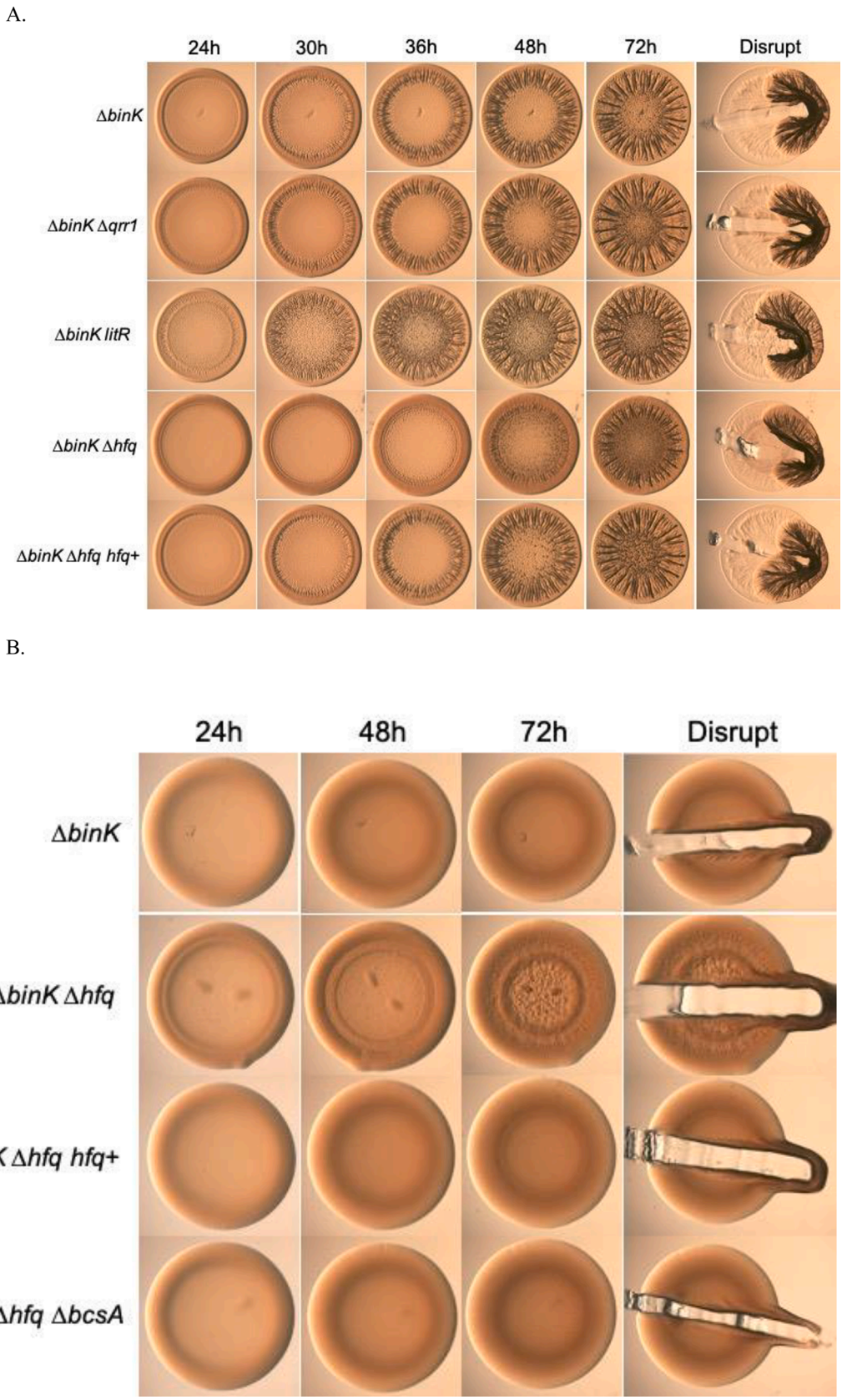

Fig. 11. Role of Hfq in biofilm formation of *V. fischeri*. The wrinkled colony assay was performed by spotting cultures of various strains on LBS with (A) or without (B) 10 mM calcium chloride, and incubating them at 24 °C. The strains pictured are (A) Δ*binK* (KV7860), Δ*binK* Δ*qrr1* (KV9347), Δ*binK litR* (KV9444), Δ*binK* Δ*hfq* (KV9069), and Δ*binK* Δ*hfq hfq*$^{+}$ (KV9075) for the calcium condition and (B) Δ*binK* (KV7860), Δ*binK* Δ*hfq* (KV9069), Δ*binK* Δ*hfq hfq*$^{+}$ (KV9075), and Δ*binK* Δ*hfq* Δ*bcsA* (KV9445) in the no calcium condition. Spots were visualized at the indicated time points using the Zeiss Stemi 2000-c microscope and a Jenoptik Gryphax Subra camera. "Disrupt" refers to the disruption of the spots using a toothpick at 72 h.

3.9. Hfq inhibits cellulose production

The data presented in Fig. 11A were generated in the presence of calcium, a necessary signal for biofilm formation by the *binK* mutant. In the absence of calcium, as expected, none of the strains formed cohesive wrinkled colonies (Fig. 11B and Supp. Fig. 2). However, we found that the Δ*hfq* derivative exhibited some colony architecture not observed for the *binK* mutant parent: the colony was bumpy rather than smooth (Fig. 11B). The bumpy architecture did not correspond to cohesiveness, as evidenced by the easy disruption of the colony (last panel of Fig. 11B). Thus, we hypothesized that the colony architecture was due to cellulose rather than to SYP (Tischler et al., 2018).

To determine if Hfq contributes to the control of cellulose production, we assessed colony color on Congo red medium. In *V. fischeri*, cellulose is a product of the *bcs* locus and a strain that lacks the *bcsA* gene appears beige on Congo red medium. In contrast, the wild-type strain

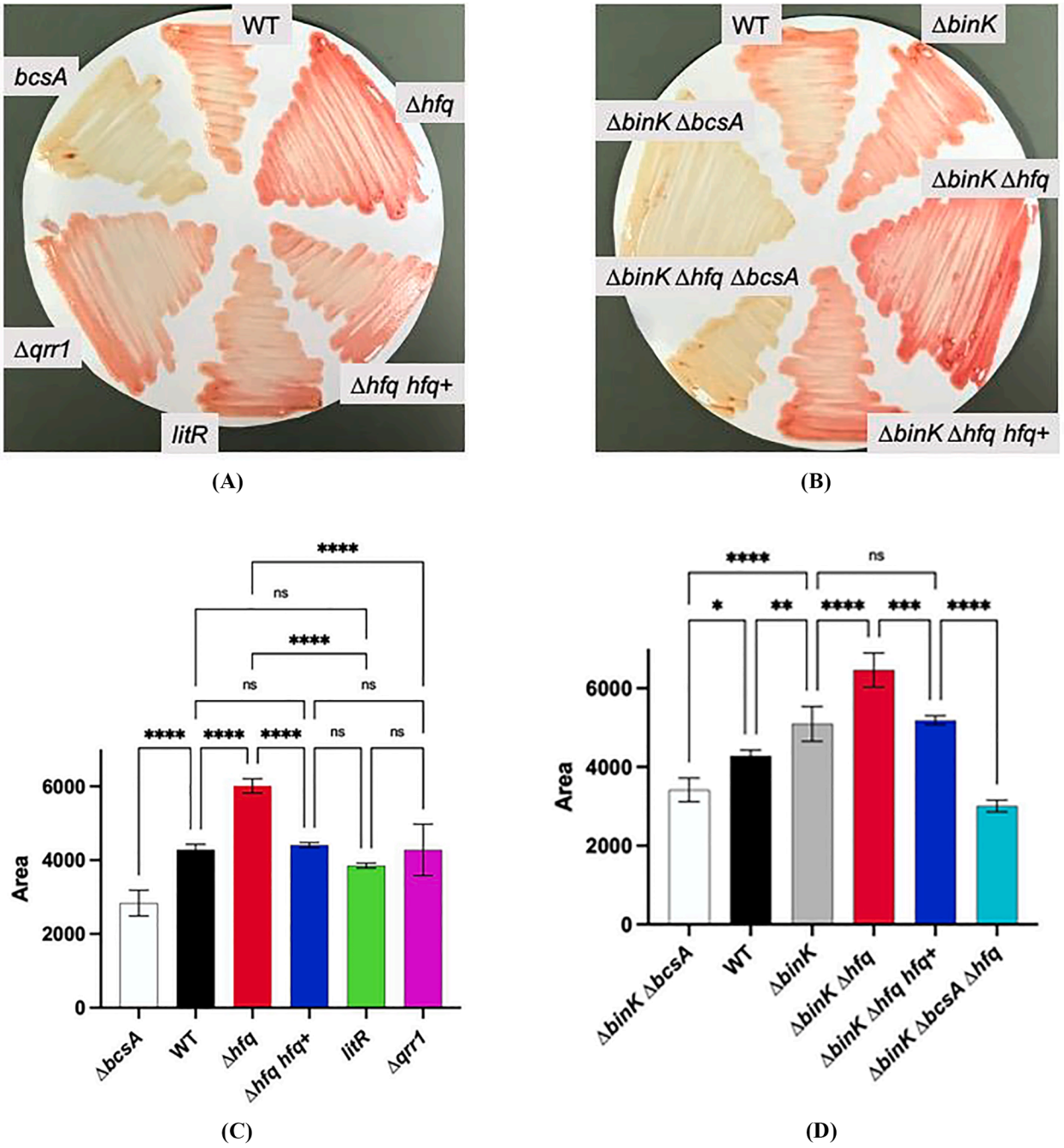

Fig. 12. Congo red assay reveals cellulose regulation by Hfq in *V. fischeri*. Strains were streaked onto LBS congo red plates to analyze their ability to bind Congo red, an indirect measure of cellulose production. After 24 h at 24 °C, the streaks were transferred to paper for better visualization. Wild-type-derived (A) and Δ*binK*-derived strains (B) are shown as follows in a clockwise direction: (left): WT (wild-type strain ES114), Δ*hfq* (KV9050), Δ*hfq hfq*$^{+}$ (KV9072), *litR* (KV6647), Δ*qrr1* (KV6678), and *bcsA* (KV8408). (right) WT (wild-type strain ES114), Δ*binK* (KV7860), Δ*binK* Δ*hfq* (KV9069), Δ*binK* Δ*hfq hfq*$^{+}$ (KV9075), and Δ*binK* Δ*hfq* Δ*bcsA* (KV9445), and Δ*binK* Δ*bcsA* (KV7908). (Wild-type ES114 is included on both plates as an internal control.) (C) and (D) are quantifications of color produced by the same strains as shown in (A) and (B), respectively, but spotted onto plates rather than streaked, as shown in Supp. Fig. 3 and processed as described in Materials and Methods. One-way ANOVA was used to compare the means of area for different strains (ns, no significant difference; *, $p < 0.05$; **, $p < 0.01$; ****, $p < 0.001$). (For interpretation of the references to color in this figure legend, the reader is referred to the web version of this article.)

produces cellulose and thus appears red (Fig. 12A and C). Deletion of *hfq* resulted in a brighter red appearance of the streak on Congo red, which was restored to the level of the wild-type by complementation with *hfq* gene. Unlike deletion of *hfq,* which results in increased cellulose production as measured by this assay, loss of *qrr1* and *litR* did not affect the amount of cellulose, as these strains appear comparable in color to the wild-type strain (Fig. 12A and C).

For a further verification that the Hfq-dependent colony architecture on medium lacking calcium (Fig. 11B) was due to the cellulose, we generated a triple *binK hfq bcsA* mutant and tested its behavior in (A) the Congo red assay and (B) colony architecture in the wrinkled colony assay. In the Congo red assay, the *hfq* and *binK hfq* mutants produced colonies with a brighter red hue relative to their respective WT and *binK* mutant parents. The colony color was restored to the parental color upon complementation (Fig. 12B and D). The triple *binK hfq bcsA* mutant appeared indistinguishable from the *binK bcsA* double mutant. This suggests that the Congo red phenotype of the *binK hfq* double mutant is due to the role of Hfq in controlling cellulose production. Correspondingly, when we evaluated colony architecture of these strains without calcium, unlike its *binK hfq* parent, the *bcsA* derivative exhibited smooth colony architecture similar to the *binK* single mutant (Fig. 11B), indicating that the bumpy colony architecture was dependent on cellulose production. Together, these data identify a novel phenotype for Hfq in controlling cellulose production.

4. Discussion

As a global regulator, Hfq contributes to a range of key functions, such as bacterial response to stress, virulence of pathogens, and group behaviors (*i.e.*, bioluminescence and biofilm formation), among others. While these contributions of Hfq have been examined in Gram-negative and Gram-positive model species, and include some commonalities as well as differences, the role of Hfq in regulating key functions of the marine bacterium *V. fischeri* has not been directly investigated. In this study, we contribute to the understanding of *V. fischeri* regulatory networks by identifying Hfq as a negative regulator of bioluminescence and a positive regulator of motility and biofilm formation. Specifically, we show that the chaperone acts along with- and independently of- known regulators of these processes, Qrr1 and LitR.

The regulatory role of Hfq in the bioluminescence pathway of *V. fischeri* has thus far only been presumed, based on the similarity of the function of the Qrr1 sRNA from *V. fischeri* to Qrr (and correspondingly Hfq) function in other *Vibrios* (Lenz et al., 2004; Miyashiro et al., 2010; Tu and Bassler, 2007). Here, we confirm that Hfq acts as a repressor of bioluminescence in *V. fischeri* (Fig. 4 and Supp. Fig. 4) and also uncover a Qrr1-independent role for Hfq in the control of light production (Fig. 5). While Hfq may assist Qrr1 in repressing *litR* mRNA translation, the tenfold increase in luminescence of the Δ*hfq* and Δ*hfq* Δ*qrr1* strains relative to the Δ*qrr1* mutant suggested that additional sRNA(s) may be controlled by Hfq. It is not unprecedented for the Hfq chaperone to be used by multiple sRNAs in regulating a single pathway, including the regulation of LitR homologue HapR in other *Vibrios* (Melamed et al., 2020; Beisel et al., 2012; Iosub et al., 2020), which may be the case for the control of bioluminescence in *V. fischeri*. In a recent report (Moriano-Gutierrez et al., 2020), an RNA-seq analysis identified six sRNAs in the *V. fischeri* outer membrane vesicles and also in the hemolymph of the squid host. Four of the six sRNAs examined have specific protein chaperones distinct from Hfq, and the remaining two were present in relatively small percentages. While this work did not specifically focus on the role of these sRNAs in luminescence it affirms our hypothesis that additional, yet to be identified, sRNAs partner with Hfq to control bioluminescence and ultimately symbiosis.

Moreover, our epistasis experiments demonstrated that an additional sRNA partner must have a target that is distinct from *litR*, the target of Qrr1. Given the increased luminescence phenotype of the *hfq* mutant and the known function of Hfq, we hypothesized that Hfq (and an unknown sRNA) either represses an activator of luminescence (similar to its effect on LitR) or activates a repressor. We tested one such possible target, the response regulator ArcA, an important bioluminescence repressor in *V. fischeri*. We expected that, if Hfq inhibits luminescence by activating the ArcA repressor, then there would be no additional consequence of deleting *hfq* in the context of an *arcA* or *arcA litR* double mutant. However, this was not the case, a result that indicated that Hfq does not exert its activity through ArcA. While these data confirmed that this sRNA chaperone works on an additional target to inhibit bioluminescence, positioning Hfq in two distinct locations in bioluminescence control (Fig. 1A), the identity of the additional target(s) remains to be determined. Additional regulators are known to control luminescence, acting outside of the established phosphorelay. For example, Hfq could inhibit the autoinducer synthase AinS, a positive regulator that produces C8-HSL autoinducer. C8-HSL works both via the phosphorelay to indirectly control LitR and by directly binding to and activating LuxR, the proximal luminescence regulator (Lyell et al., 2013). Repression of AinS production (and thus C8-HSL synthesis) would lead to decreased luminescence that is independent of Qrr1-mediated repression of LitR. Alternatively, Hfq could inhibit the expression of cyclic-AMP receptor protein (CRP), which is a known regulator of *lux* (Lyell et al., 2013) and also a known regulator of metabolism. A *crp* deletion mutant of *V. fischeri* exhibited a two-log decrease in luminescence compared to ES114 (Colton and Stabb, 2016), which is the equivalent to the increase in luminescence caused by the loss of *hfq* (Fig. 5). It is thus formally possible that Hfq indirectly controls luminescence by regulating CRP. Finally, Hfq may impact an as-yet unknown luminescence regulator. Further genetic and epistatic analysis will be necessary to identify the additional luminescence-relevant target(s) of Hfq in *V. fischeri.*

The contribution of Hfq to the regulation of motility has been appreciated for some time in *E. coli* and *Salmonella enterica servovar* Typhimurium; this is mostly based on the findings that Hfq-dependent sRNAs regulate expression of flagellar genes (De Lay and Gottesman, 2012; Sittka et al., 2007; Romilly et al., 2020). We show that Hfq promotes motility in *V. fischeri* and that it does so in a manner that is partially independent of Qrr1 and LitR (Figs. 9 and 10). Previous work has found LitR to be a negative regulator of motility (Lupp and Ruby, 2005), although under our assay conditions the *litR* mutant did not show a significant difference in motility from the wild type strain as was reported by Fidopiastis *et al.* (Fidopiastis et al., 2002) and by Dial *et al.* (Dial et al., 2021); however, its role as a negative regulator was clear from our epistasis analyses. The regulation by Hfq in the motility pathway appears to be in the opposite direction from its role in controlling bioluminescence where Hfq acts as a repressor. As in the bioluminescence regulatory pathway, the contribution of Hfq appears to be greater than that of Qrr1 sRNA (Fig. 10), which suggests a role for an as yet un-identified sRNA (or multiple sRNAs) that operates under Hfq guidance. In bacterial species where regulation of flagellar-based motility has been examined at the post-transcriptional level, it has been determined to be dependent on multiple sRNAs (De Lay and Gottesman, 2012; Romilly et al., 2020; Schachterle Jeffrey et al., 2019). Thus, it will be of interest to determine if the Hfq-dependent sRNA (other than Qrr1) that functions in luminescence control is the same one involved in the regulation of motility in *V. fischeri.*

The number of sRNAs that require Hfq for proper target regulation in *E. coli* is on the order of several hundred (Gottesman and Storz, 2011; Hör et al., 2018; Vogel and Luisi, 2011). There are, for example, multiple sRNAs interacting with Hfq that affect motility (i.e. ArcZ, OmrA/B, OxyS, McaS, MicA) in *E. coli* (De Lay and Gottesman, 2012), but the homologs of these are not easily identifiable in the genome of *V. fischeri.* In addition to Hfq, another sRNA chaperone, ProQ, has recently been determined to have both an overlapping and a distinct set of sRNAs with which it post-transcriptionally affects targets controlled by Hfq (Melamed et al., 2020; Olejniczak and Storz, 2017; Attaiech et al., 2017). Whether the same is true for *V. fischeri* remains unknown, although a putative *proQ* gene exists in the genome. A global analysis of sRNAs,

their chaperones and mRNA targets would help illuminate the similarities and differences between *V. fischeri* and other Gram-negative bacteria for which this has already been determined.

Similar to what we found for the regulation of motility in *V. fischeri*, Hfq also positively regulates *syp*-dependent biofilm formation (Fig. 11). Specifically, Hfq plays a substantial role in promoting the development of wrinkled colonies, although sticky, SYP-dependent colonies can form in the absence of Hfq. This chaperone also negatively controls the cellulose component of the biofilm: in the absence of the biofilm-inducing signal calcium, the biofilm-competent parent strain fails to form a biofilm, while the Δ*hfq* derivative produced colonies with architecture, but lacking stickiness. This phenotype is consistent with that of a cellulose-dependent biofilm (Tischler et al., 2018; Visick et al., 2018), and indeed, was disrupted when cellulose-production components were also eliminated (Fig. 11B). Furthermore, the Δ*hfq* mutant exhibited a cellulose-dependent increase in binding to Congo Red relative to the wild-type strain (Fig. 12). This role for Hfq in controlling cellulose coincides with what has been reported for enteric pathogens where the expression of curli, extracellular proteinaceous structures (Barnhart and Chapman, 2006; Holmqvist et al., 2010) and cellulose important for biofilm formation, have been found to be post-transcriptionally controlled by several sRNAs. In addition to ascribing a role for Hfq in control of cellulose-dependent biofilms, we have also uncovered a previously unknown contribution of LitR as a repressor of SYP-dependent biofilms in *V. fischeri* (Fig. 11A). While the opposite effects of Hfq and LitR on biofilms are not surprising, the same direction (i.e., repression) of regulation by LitR and Qrr1 is. Since Qrr1 is a repressor of LitR (Fig. 1B), we would expect that the phenotypes of the strains that lack these regulators would produce opposite phenotypes, but they both resulted in earlier and more robust biofilms than the parent strain (Fig. 11A). An explanation for this may be that additional regulators control the function of LitR in the biofilm pathway. Recently, a novel LitR regulator in *V. fischeri,* HbtR, a homolog of *V. cholerae* virulence factor TcpP, has been described (Bennett et al., 2020). The contribution of this regulator to biofilm formation, however, remains to be investigated.

An examination of the protein sequence of *V. fischeri* Hfq and comparison with that of *E. coli* revealed a high level of identity, with the major difference being a shorter C-terminal region in *V. fischeri* (Fig. 2A). *Pseudomonas aeruginosa* also encodes an Hfq that lacks the C-terminal amino acids found in *E. coli*, yet this protein was able to functionally replace the *E. coli* Hfq (Sonnleitner et al., 2002), indicating that the functional domain of Hfq resides in the N-terminus. The stretch of approximately 12 amino acids that is found in *E. coli* Hfq C-terminus (and absent from Hfq of the *Vibrios*) is thought to contribute to nucleic acid binding, but until recently its structure had remained elusive (Fortas et al., 2015; Santiago-Frangos et al., 2016; Sharma et al., 2018). A comparison of the Hfq proteins from *E. coli* and *V. cholerae* using biochemical and biophysical approaches has shown that, despite the similarity in structure and ability to bind to Qrr sRNA, there is a difference in the stability of the hexamers (Vincent et al., 2012). It was proposed that this is due to the difference in the subunit interface and that the higher stability of the *E. coli* Hfq is mediated by the longer C-terminal domain (Vincent et al., 2012). A new and unique role for the C-terminus of Hfq was proposed when it was found to interact with lipid bilayers and liposomes, suggesting that the chaperone may be involved in accompanying sRNAs outside of the cell (Malabirade et al., 2017). It would be of interest to determine whether Hfq of *Vibrios* could accomplish this task in the absence of the C-terminal tail, since it has been reported that outer membrane vesicles influence *V. fischeri*'s interaction with its symbiotic host (Moriano-Gutierrez et al., 2020).

In conclusion, we ascribe to Hfq roles in the regulation of growth, bioluminescence, motility, and biofilm formation in *V. fischeri*. Based on our epistatic analysis, we can place the chaperone in previously described pathways (Fig. 1), where its role had only been postulated, and in another unknown pathway(s) controlling these processes. Thus, our work contributes towards a greater understanding of the complexity of regulatory networks that integrate environmental cues and allow *V. fischeri* to establish a productive symbiosis with the squid host.

Declaration of Competing Interest

The authors declare no financial interestes/personal relationships which may be considered as potential competing interests.

Acknowledgements

This work was supported by Wheaton College Aldeen Grants (JT) and NIH General Medical Sciences grants R01 GM114288 and R35 GM130355 (KV). The authors thank previous members of Tepavcevic lab, current and present members of the Visick lab, and students in Biol252 course at Wheaton College for helpful discussion.

Appendix A. Supplementary material

Supplementary data to this article can be found online at https://doi.org/10.1016/j.gene.2021.146048.

References

Arce-Rodríguez, A., Calles, B., Nikel, P.I., de Lorenzo, V., 2016. The RNA chaperone Hfq enables the environmental stress tolerance super-phenotype of *Pseudomonas putida*. Environ. Microbiol. 18 (10), 3309–3326.

Attaiech, L., Glover, J.N.M., Charpentier, X., 2017. RNA chaperones step out of Hfq's shadow. Trends Microbiol. 25 (4), 247–249.

Bai, G., Golubov, A., Smith, E.A., McDonough, K.A., 2010. The importance of the small RNA chaperone Hfq for growth of epidemic *Yersinia pestis*, but not *Yersinia pseudotuberculosis*, with implications for plague biology. J. Bacteriol. 192, 4239.

Bardill, J.P., Zhao, X., Hammer, B.K., 2011. The *Vibrio cholerae* quorum sensing response is mediated by Hfq-dependent sRNA/mRNA base pairing interactions. Mol. Microbiol. 80, 1381–1394.

Barnhart, M.M., Chapman, M.R., 2006. Curli biogenesis and function. Annu. Rev. Microbiol. 60 (1), 131–147.

Beisel, C.L., Updegrove, T.B., Janson, B.J., Storz, G., 2012. Multiple factors dictate target selection by Hfq-binding small RNAs. EMBO J. 2012 (31), 1961–1974.

Bellows, L.E., Koestler, B.J., Karaba, S.M., Waters, C.M., Lathem, W.W., 2012. Hfq-dependent, co-ordinate control of cyclic diguanylate synthesis and catabolism in the plague pathogen *Yersinia pestis*. Mol. Microbiol. 86 (3), 661–674.

Bennett, B.D., Essock-Burns, T., Ruby, E.G., 2020. HbtR, a heterofunctional homolog of the virulence regulator TcpP, facilitates the transition between symbiotic and planktonic lifestyles in *Vibrio fischeri*. mBio 11, e01624–20.

Bjelland, A.M., Sørum, H., Tegegne, D.A., Winther-Larsen, H.C., Willassen, N.P., Hansen, H., Camilli, A., 2012. LitR of *Vibrio salmonicida* is a salinity-sensitive quorum-sensing regulator of phenotypes involved in host interactions and virulence. Infect. Immun. 80 (5), 1681–1689.

Boettcher, K.J., Ruby, E.G., 1990. Depressed light emission by symbiotic *Vibrio fischeri* of the sepiolid squid *Euprymna scolopes*. J. Bacteriol. 172 (7), 3701–3706.

Bose, J.L., Kim, U., Bartkowski, W., Gunsalus, R.P., Overley, A.M., Lyell, N.L., Visick, K. L., Stabb, E.V., 2007. Bioluminescence in *Vibrio fischeri* is controlled by the redox-responsive regulator ArcA. Mol. Microbiol. 65 (2), 538–553.

Brooks, J.F., Gyllborg, M.C., Cronin, D.C., Quillin, S.J., Mallama, C.A., Foxall, R., Whistler, C., Goodman, A.L., Mandel, M.J., 2014. Global discovery of colonization determinants in the squid symbiont *Vibrio fischeri*. Proc. Natl. Acad. Sci. 111 (48), 17284–17289.

Brooks, J.F., Mandel, M.J., O'Toole, G.A., 2016. The histidine kinase BinK Is a negative regulator of biofilm formation and squid colonization. J. Bacteriol. 198 (19), 2596–2607.

Christensen, D.G., Tepavčević, J., Visick, K.L., 2020. Genetic manipulation of *Vibrio fischeri*. Curr. Protoc. Microbiol. 59 (1), e.115.

Christiansen, J.K., Larsen, M.H., Ingmer, H., Søgaard-Andersen, L., Kallipolitis, B.H., 2004. The RNA-binding protein Hfq of *Listeria monocytogenes*: role in stress tolerance and virulence. J. Bacteriol. 186 (11), 3355–3362.

Colton, D.M., Stabb, E.V., 2016. Rethinking the roles of CRP, cAMP, and sugar-mediated global regulation in the *Vibrionaceae*. Curr. Genet. 62 (1), 39–45.

Davis, R., Botstein, D., Roth, J., 1980. Advanced Bacterial Genetics. Cold Spring Har-bor Laboratory, N Y.

De Lay, N., Gottesman, S., 2012. A complex network of small non-coding RNAs regulate motility in *Escherichia coli*. Mol. Microbiol. 86 (3), 524–538.

DeLoney-Marino, C.R., Wolfe, A.J., Visick, K.L., 2003. Chemoattraction of *Vibrio fischeri* to serine, nucleosides, and acetylneuraminic acid, a component of squid light-organ mucus. Appl. Environ. Microbiol. 69, 7527.

Deng, Y., Chen, C., Zhao, Z., Zhao, J., Jacq, A., Huang, X., Yang, Y., 2016. The RNA chaperone Hfq is involved in colony morphology, nutrient utilization and oxidative and envelope stress response in *Vibrio alginolyticus*. PLoS ONE 11, e0163689.

Dereeper, A., Guignon, V., Blanc, G., Audic, S., Buffet, S., Chevenet, F., Dufayard, J.-F., Guindon, S., Lefort, V., Lescot, M., Claverie, J.-M., Gascuel, O., 2008. Phylogeny.fr:

robust phylogenetic analysis for the non-specialist. Nucleic Acids Res. 36 (Web Server), W465–W469.
Dial, C.N., Eichinger, S.J., Foxall, R., Corcoran, C.J., Tischler, A.H., Bolz, R.M., Whistler, C.A., Visick, K.L., 2021. Quorum sensing and cyclic di-GMP exert control over motility of *Vibrio fischeri* KB2B1. Front. Microbiol. 12.
Fidopiastis, P.M., Miyamoto, C.M., Jobling, M.G., Meighen, E.A., Ruby, E.G., 2002. LitR, a new transcriptional activator in *Vibrio fischeri*, regulates luminescence and symbiotic light organ colonization. Mol. Microbiol. 45 (1), 131–143.
Fortas, E., Piccirilli, F., Malabirade, A., Militello, V., Trépout, S., Marco, S., Taghbalout, A., Arluison, V., 2015. New insight into the structure and function of Hfq C-terminus. Biosci. Rep. 35.
Gottesman, S., Storz, G., 2011. Bacterial small RNA regulators: versatile roles and rapidly evolving variations. Cold Spring Harb Perspect. Biol. 3.
Han, K., Tjaden, B., Lory, S., 2016. GRIL-seq provides a method for identifying direct targets of bacterial small regulatory RNA by in vivo proximity ligation. Nat. Microbiol. 2, 16239.
Hansen, H., Bjelland, A.M., Ronessen, M., Robertsen, E., Willassen, N.P., 2014. LitR is a repressor of *syp* genes and has a temperature-sensitive regulatory effect on biofilm formation and colony morphology in *Vibrio* (*Aliivibrio*) *salmonicida.* Appl. Environ. Microbiol., 2014/06/27 ed. 80:5530–5541.
Holmqvist, E., Reimegård, J., Sterk, M., Grantcharova, N., Römling, U., Wagner, E.G.H., 2010. Two antisense RNAs target the transcriptional regulator CsgD to inhibit curli synthesis. EMBO J. 29 (11), 1840–1850.
Hör, J., Gorski, S.A., Vogel, J., 2018. Bacterial RNA biology on a genome scale. Mol. Cell 70 (5), 785–799.
Ikeda, Y., Yagi, M., Morita, T., Aiba, H., 2011. Hfq binding at RhlB-recognition region of RNase E is crucial for the rapid degradation of target mRNAs mediated by sRNAs in *Escherichia coli*. Mol. Microbiol. 79, 419–432.
Iosub, I.A., van Nues, R.W., McKellar, S.W., Nieken, K.J., Marchioretto, M., Sy, B., Tree, J.J., Viero, G., Granneman, S., 2020. Hfq CLASH uncovers sRNA-target interaction networks linked to nutrient availability adaptation. eLife 9.
Kavita, K., de Mets, F., Gottesman, S., 2018. New aspects of RNA-based regulation by Hfq and its partner sRNAs. Cell Regul 42, 53–61.
Kimbrough, J.H., Stabb, E.V., O'Toole, G.A., 2016. Antisocial *luxO* Mutants Provide a Stationary-Phase Survival Advantage in *Vibrio fischeri* ES114. J. Bacteriol. 198 (4), 673–687.
King, A.M., Vanderpool, C.K., Degnan, P.H., Ellermeier, C.D., 2019. sRNA target prediction organizing tool (SPOT) integrates computational and experimental data to facilitate functional characterization of bacterial small RNAs. mSphere 4 (1). https://doi.org/10.1128/mSphere.00561-18.
Lalaouna, D., Morissette, A., Carrier, M.-C., Massé, E., 2015. DsrA regulatory RNA represses both *hns* and *rbsD* mRNAs through distinct mechanisms in *Escherichia coli*. Mol. Microbiol. 98 (2), 357–369.
Lenz, D.H., Mok, K.C., Lilley, B.N., Kulkarni, R.V., Wingreen, N.S., Bassler, B.L., 2004. The small RNA chaperone Hfq and multiple small RNAs control quorum sensing in *Vibrio harveyi* and *Vibrio cholerae*. Cell 118 (1), 69–82.
Liu, X., Yan, Y., Wu, H., Zhou, C., Wang, X., 2019. Biological and transcriptomic studies reveal *hfq* is required for swimming, biofilm formation and stress response in *Xanthomonas axonpodis* pv. citri. BMC Microbiol. 19 (103).
Livak, K.J., Schmittgen, T.D., 2001. Analysis of relative gene expression data using real-time quantitative PCR and the $2-\Delta\Delta CT$ method. Methods 25 (4), 402–408.
Lupp, C., Ruby, E.G., 2005. *Vibrio fischeri* uses two quorum-sensing systems for the regulation of early and late colonization factors. J. Bacteriol. 187 (11), 3620–3629.
Lyell, N.L., Dunn, A.K., Bose, J.L., Stabb, E.V., 2010. Bright mutants of *Vibrio fischeri* ES114 reveal conditions and regulators that control bioluminescence and expression of the lux operon. J. Bacteriol. 192 (19), 5103–5114.
Lyell, N.L., Colton, D.M., Bose, J.L., Tumen-Velasquez, M.P., Kimbrough, J.H., Stabb, E. V., 2013. Cyclic AMP receptor protein regulates pheromone-mediated bioluminescence at multiple levels in *Vibrio fischeri* ES114. J. Bacteriol. 195 (22), 5051–5063.
Madeira, F., Park, Y.M., Lee, J., Buso, N., Gur, T., Madhusoodanan, N., Basutkar, P., Tivey, A.R.N., Potter, S.C., Finn, R.D., Lopez, R.. 2019. The EMBL-EBI search and sequence analysis tools APIs in 2019. Nucleic Acids Res 47:W636–W641.
Malabirade, A., Morgado-Brajones, J., Trépout, S., Wien, F., Marquez, I., Seguin, J., Marco, S., Velez, M., Arluison, V., 2017. Membrane association of the bacterial riboregulator Hfq and functional perspectives. Sci. Rep. 7, 10724.
Mandel, M.J., Dunn, A.K., 2016. Impact and influence of the natural vibrio-squid symbiosis in understanding bacterial-animal interactions. Front. Microbiol. 7, 1982.
Melamed, S., Adams, P.P., Zhang, A., Zhang, H., Storz, G., 2020. RNA-RNA interactomes of ProQ and Hfq reveal overlapping and competing roles. Mol. Cell 77 (2), 411–425. e7.
Miyashiro, T., Ruby, E.G., 2012. Shedding light on bioluminescence regulation in *Vibrio fischeri*. Mol Microbiol 84:795–806.
Miyashiro, T., Wollenberg, M.S., Cao, X., Oehlert, D., Ruby, E.G., 2010. A single *qrr* gene is necessary and sufficient for LuxO-mediated regulation in *Vibrio fischeri*. Mol. Microbiol. 77, 1556–1567.
Moriano-Gutierrez, S., Bongrand, C., Essock-Burns, T., Wu, L., McFall-Ngai, M.J., Ruby, E.G., Teixeira, L., 2020. The noncoding small RNA SsrA is released by *Vibrio fischeri* and modulates critical host responses. PLoS Biol. 18 (11), e3000934.
Norsworthy, A., Visick, K., 2013. Gimme shelter: how *Vibrio fischeri* successfully navigates an animal's multiple environments. Front. Microbiol. 4, 356.
Olejniczak, M., Storz, G., 2017. ProQ/FinO-domain proteins: another ubiquitous family of RNA matchmakers? Mol. Microbiol. 104 (6), 905–915.
Parker, A., Cureoglu, S., De Lay, N., Majdalani, N., Gottesman, S., 2017. Alternative pathways for *Escherichia coli* biofilm formation revealed by sRNA overproduction. Mol. Microbiol. 105 (2), 309–325.
Prévost, K., Desnoyers, G., Jacques, J.-F., Lavoie, F., Massé, E., 2011. Small RNA-induced mRNA degradation achieved through both translation block and activated cleavage. Genes Dev., 2011/02/02 ed. 25:385–396.
Ray, V.A., Morris, A.R., Visick, K.L., 2012. A semi-quantitative approach to assess biofilm formation using wrinkled colony development. J. Vis. Exp. JoVE e4035–e4035.
Robertson, G.T., Roop, R.M., 1999. The Brucella abortus host factor I (HF-I) protein contributes to stress resistance during stationary phase and is a major determinant of virulence in mice. Mol. Microbiol. 34 (4), 690–700.
Romilly, C., Hoekzema, M., Holmqvist, E., Wagner, E.G.H., 2020. Small RNAs OmrA and OmrB promote class III flagellar gene expression by inhibiting the synthesis of anti-Sigma factor FlgM. RNA Biol. 17 (6), 872–880.
Santiago-Frangos, A., Kavita, K., Schu, D.J., Gottesman, S., Woodson, S.A., 2016. C-terminal domain of the RNA chaperone Hfq drives sRNA competition and release of target RNA. Proc. Natl. Acad. Sci. 113 (41), E6089–E6096.
Septer, A.N., Stabb, E.V., Liles, M.R., 2012. Coordination of the arc regulatory system and pheromone-mediated positive feedback in controlling the *Vibrio fischeri lux* operon. PLoS ONE 7 (11), e49590.
Schachterle Jeffrey, K., Zeng, Q., Sundin, G.W., 2019. Three Hfq-dependent small RNAs regulate flagellar motility in the fire blight pathogen *Erwinia amylovora*. Mol Microbiol. 14232.
Septer, A.N., Lyell, N.L., Stabb, E.V., 2013. The iron-dependent regulator fur controls pheromone signaling systems and luminescence in the squid symbiont *Vibrio fischeri* ES114. Appl. Environ. Microbiol. 79 (6), 1826–1834.
Sharma, A., Dubey, V., Sharma, R., Devnath, K., Gupta, V.K., Akhter, J., Bhando, T., Verma, A., Ambatipudi, K., Sarkar, M., Pathania, R., 2018. The unusual glycine-rich C terminus of the *Acinetobacter baumannii* RNA chaperone Hfq plays an important role in bacterial physiology. J. Biol. Chem. 2018 (293), 13377–13388.
Sievers, F., Wilm, A., Dineen, D., Gibson, T.J., Karplus, K., Li, W., Lopez, R., McWilliam, H., Remmert, M., Söding, J., Thompson, J.D., Higgins, D.G., 2011. Fast, scalable generation of high-quality protein multiple sequence alignments using Clustal Omega. Mol. Syst. Biol. 7, 539.
Sittka, A., Pfeiffer, V., Tedin, K., Vogel, J., 2007. The RNA chaperone Hfq is essential for the virulence of *Salmonella typhimurium*. Mol. Microbiol. 63 (1), 193–217.
Sonnleitner, E., Moll, I., Bläsi, U., 2002. Functional replacement of the *Escherichia coli hfq* gene by the homologue of *Pseudomonas aeruginosa*. Microbiol. Microbiol. Soc.
Soper, T., Mandin, P., Majdalani, N., Gottesman, S., Woodson, S.A., 2010. Positive regulation by small RNAs and the role of Hfq. Proc. Natl. Acad. Sci. 107 (21), 9602–9607.
Stabb, E.V., Reich, K.A., Ruby, E.G., 2001. *Vibrio fischeri* Genes *hvnA* and *hvnB* encode secreted NAD+-glycohydrolases. J. Bacteriol. 183 (1), 309–317.
Thompson, C.M., Tischler, A.H., Tarnowski, D.A., Mandel, M.J., Visick, K.L., 2019. Nitric oxide inhibits biofilm formation by *Vibrio fischeri* via the nitric oxide sensor HnoX. Mol. Microbiol. 111 (1), 187–203.
Tischler, A.H., Lie, L., Thompson, C.M., Visick, K.L., O'Toole, G., 2018. Discovery of calcium as a biofilm-promoting signal for *Vibrio fischeri* reveals new phenotypes and underlying regulatory complexity. J. Bacteriol. 200 (15) https://doi.org/10.1128/JB.00016-18.
Tsui, H.-C., Leung, H.-C., Winkler, M.E., 1994. Characterization of broadly pleiotropic phenotypes caused by an *hfq* insertion mutation in *Escherichia coli* K-12. Mol. Microbiol. 13 (1), 35–49.
Tu, K.C., Bassler, B.L., 2007. Multiple small RNAs act additively to integrate sensory information and control quorum sensing in *Vibrio harveyi*. Genes Dev., 21:221–233.
Verma, S.C., Miyashiro, T., 2013. Quorum sensing in the squid-*Vibrio* symbiosis. Int. J. Mol. Sci. 14 (8), 16386–16401.
Vincent, H.A., Henderson, C.A., Ragan, T.J., Garza-Garcia, A., Cary, P.D., Gowers, D.M., Malfois, M., Driscoll, P.C., Sobott, F., Callaghan, A.J., 2012. Characterization of *Vibrio cholerae* Hfq provides novel insights into the role of the Hfq C-terminal region. J. Mol. Biol. 420 (1-2), 56–69.
Visick, K.L., 2009. An intricate network of regulators controls biofilm formation and colonization by *Vibrio fischeri*. Mol. Microbiol. 74, 782–789.
Visick, K.L., Hodge-Hanson, K.M., Tischler, A.H., Bennett, A.K., Mastrodomenico, V., Atomi, H., 2018. Tools for Rapid Genetic Engineering of *Vibrio fischeri*. Appl. Environ. Microbiol. 84 (14) e00850-18.
Visick, K.L., Stabb, E.V., Ruby, E.G., 2021. A lasting symbiosis: how *Vibrio fischeri* finds a squid partner and persists within its natural host. Nat. Rev. Microbiol. 19 (10), 654–665.
Vogel, J., Luisi, B.F., 2011. Hfq and its constellation of RNA. Nat. Rev. Microbiol. 9 (8), 578–589.
Yao, H., Kang, M., Wang, Y., Feng, Y., Kong, S., Cai, X., Ling, Z., Chen, S., Jiao, X., Yin, Y., 2018. An essential role for *hfq* involved in biofilm formation and virulence in serotype 4b *Listeria monocytogenes*. Microbiol. Res. 215, 148–154.
Zhao, X., Koestler, B.J., Waters, C.M., Hammer, B.K., 2013. Post-transcriptional activation of a diguanylate cyclase by quorum sensing small RNAs promotes biofilm formation in *Vibrio cholerae*. Mol. Microbiol. 89 (5), 989–1002.